Immunity, Vol. 21, 539–550, October, 2004, Copyright ©2004 by Cell Press

Osteopontin as a Mediator of NKT Cell Function in T Cell-Mediated Liver Diseases

Hongyan Diao,[1] Shigeyuki Kon,[1] Kazuya Iwabuchi,[2] Chiemi Kimura,[1] Junko Morimoto,[1] Daisuke Ito,[1] Tatsuya Segawa,[3] Masahiro Maeda,[3] Junji Hamuro,[4] Toshinori Nakayama,[5] Masaru Taniguchi,[6] Hideo Yagita,[7] Luc Van Kaer,[8] Kazunori Onóe,[2] David Denhardt,[9] Susan Rittling,[10] and Toshimitsu Uede[1,*]

[1]Division of Molecular Immunology and
[2]Division of Immunobiology
Institute for Genetic Medicine
Hokkaido University
Sapporo, 060-0815
Japan
[3]Immuno-Biological Laboratories Co., Ltd.
Gunma, 375-0005
Japan
[4]Pharmaceutical Research Laboratories
Ajinomoto Co., Inc.
Kanagawa, 210-8613
Japan
[5]Department of Immunology
Graduate School of Medicine
Chiba University
Chiba, 260-8670
Japan
[6]Laboratory of Immune Regulation
RIKEN Research Center for Allergy and Immunology
Yokohama, 230-0045
Japan
[7]Department of Immunology
Juntendo University School of Medicine
Tokyo, 113-8421
Japan
[8]Department of Microbiology and Immunology
Vanderbilt University School of Medicine
Nashville, Tennessee 37232
[9]Department of Cell Biology and Neuroscience
Rutgers University
Piscataway, New Jersey 08854
[10]Department of Genetics
Rutgers University
Piscataway, New Jersey 08855

Summary

Both osteopontin (OPN) and natural killer T (NKT) cells play a role in the development of immunological disorders. We examined a functional link between OPN and NKT cells. Concanavalin A (Con A)-induced hepatitis is a well-characterized murine model of T cell-mediated liver diseases. Here, we show that NKT cells secrete OPN, which augments NKT cell activation and triggers neutrophil infiltration and activation. Thus, OPN- and NKT cell-deficient mice were refractory to Con A-induced hepatitis. In addition, a neutralizing antibody specific for a cryptic epitope of OPN, exposed by thrombin cleavage, ameliorated hepatitis. These findings identify NKT cell-derived OPN as a novel target for the treatment of inflammatory liver diseases.

*Correspondence: toshi@igm.hokudai.ac.jp

Introduction

T cell-mediated liver diseases including autoimmune hepatitis and viral hepatitis are associated with significant morbidity and mortality worldwide and remain a serious concern in the clinical setting (Diao et al., 2001; McFarlane, 1999). Concanavalin A (Con A)-induced hepatitis in the mouse is a well-characterized model of T cell-mediated liver diseases (Tiegs et al., 1992). Following Con A administration, liver histology shows massive granulocyte accumulation, CD4 T cell infiltration, influx of a relatively small number of CD8 T cells, and hepatocyte necrosis/apoptosis (Chen et al., 2001; Tiegs et al., 1992). Previous studies have shown that various immunoregulatory cytokines play a role in the pathogenesis of Con A-induced hepatitis. Th1 type cytokines such as interferon (IFN)-γ, interleukin (IL)-12, and tumor necrosis factor (TNF)-α promote liver injury, whereas the Th2 type cytokine IL-10 suppresses liver injury (Kaneko et al., 2000; Louis et al., 1997).

Recent studies have implicated hepatic NKT cells in the development of Con A-induced hepatitis. Both Jα18- and CD1d-deficient mice that lack NKT cells are resistant to Con A-induced hepatic injury (Kaneko et al., 2000; Takeda et al., 2000), indicating that classical CD1d-restricted NKT cells that express the invariant Vα14-Jα18 T cell receptor are critically involved in the process of Con A-induced hepatic injury. Upon activation, NKT cells secrete various cytokines (e.g., IFN-γ) that activate resident Kupffer cells and recruit macrophages to produce TNF-α, which subsequently causes liver injury (Burdin et al., 1998; Takeda et al., 2000). Additionally, the Th2 type cytokine IL-4 causes NKT cells to express Fas ligand (FasL), contributing to Fas/FasL-mediated liver injury in an autocrine fashion (Takeda et al., 2000). However, how activation of NKT cells leads to hepatic injury remains to be fully elucidated.

It is known that a variety of inflammatory and autoimmune diseases (including MS, RA, and atherosclerosis) are critically regulated by NKT cells (Chiba et al., 2004; Jahng et al., 2001; Tupin et al., 2004). Interestingly, each of these diseases is associated with high osteopontin (OPN) expression (Chabas et al., 2001; Matsui et al., 2003; Ohshima et al., 2002; Steinman and Zamvil, 2003). OPN is known not only as an extracellular matrix protein, supporting adhesion and migration of inflammatory cells, but also as an immunoregulatory cytokine (Ashkar et al., 2000; O'Regan et al., 2000). Furthermore, both OPN- and CD1d-deficient mice are resistant to high fat diet-induced atherosclerosis (Matsui et al., 2003; Tupin et al., 2004). Importantly, overexpression of OPN was associated with various inflammatory liver diseases (Morimoto et al., 2004; Tanaka et al., 2004). Therefore, we sought to determine whether there is any mechanistic link between OPN and NKT cells and whether OPN

contributes to Con A-induced fulminant hepatitis. Here, we show that, during Con A-induced fulminant hepatitis, NKT cells regulate the severity of neutrophil infiltration into the liver and the levels of hepatic injury by secreting OPN. Targeting this pathway holds promise for the treatment of inflammatory hepatitis.

Results

Requirement of NKT Cells and OPN in Con A-Induced Hepatic Injury

Since it has been shown that CD1d-deficient mice lacking NKT cells are protected from Con A-induced hepatitis (Takeda et al., 2000), we first compared the liver damage after Con A injection in CD1d-deficient, OPN-deficient, and wild-type mice of the C57BL/6 background. To address the role of CD1d-restricted classical NKT cells, we also injected Con A into Jα18-deficient mice. Liver damage, as reflected by serum ALT levels, peaked at 12 hr and then declined at 24 hr after Con A injection in wild-type mice. In sharp contrast, in CD1d-, Jα18- and OPN-deficient mice, ALT levels were significantly lower than those in wild-type mice. There was no significant difference in ALT levels among Con A-treated CD1d-, Jα18-, and OPN-deficient mice (Figure 1A). Consistent with the ALT levels, histological examination showed diffuse and massive degenerative liver alterations after Con A injection in wild-type mice, whereas only focal and mild liver injury was detected in OPN-, Jα18-, and CD1d-deficient mice (Figure 1B). Importantly, survival was also substantially enhanced in OPN-deficient mice (Figure 1C). We also showed that CD1d-deficient mice were well protected from death after Con A injection (Figure 1C), as previously reported (Kaneko et al., 2000). Thus either OPN deficiency or NKT cell deficiency rendered mice to be resistant to Con A-induced hepatic injury. Importantly, OPN mutant mice have no major defects in NKT cell and conventional T cell development and function, although numbers of NKT cells in the spleen and liver of these animals may be slightly reduced (data not shown).

To provide further evidence for the contribution of NKT cells and OPN to Con A-induced hepatic injury, we tested whether adoptive transfer of NKT cells from wild-type animals could render CD1d- or OPN-deficient mice susceptible to Con A-induced hepatic injury. Intrahepatic injection of C57BL/6-derived NKT ($NK1.1^+TCR^+$) cells along with Con A elevated the serum ALT levels in both CD1d- and OPN-deficient mice, whereas injection of NKT ($NK1.1^+TCR^+$) cells derived from OPN-deficient mice did not (Figure 1D). The involvement of CD1d-restricted classical NKT cells in Con A-induced hepatic injury was further tested by adoptive transfer of NKT cells purified with α-galactosylceramide (α-GC)-loaded CD1d dimers and anti-TCR antibodies. Results showed that NKT cells from wild-type, but not OPN-deficient, mice restored Con A-induced hepatic injury in OPN-deficient mice, as judged by the elevation of ALT levels in reconstituted animals (Figure 1E).

NKT Cell-Deficient Mice Are Defective in Con A-Induced OPN Production

To further investigate a mechanistic link between OPN and NKT cells in Con A-induced hepatic injury, we next examined the plasma OPN levels after Con A injection in wild-type, CD1d-, Jα18-, and OPN-deficient mice. In wild-type mice, plasma levels of OPN were significantly increased at 6 hr and further increased thereafter. In CD1d- and Jα18-deficient mice, however, plasma OPN levels were significantly lower than those in wild-type mice (Figure 2A). In addition, we injected mice with the potent NKT cell activator α-GC (Kawano et al., 1997) and found that this treatment induced a significant elevation of plasma OPN levels in wild-type mice, but not CD1d- and Jα18-deficient mice (Figure 2B). Plasma OPN was not detected after Con A (Figure 2A) or α-GC (data not shown) treatment of OPN-deficient mice.

To examine whether NKT cells could be a source of OPN, we isolated intrahepatic leukocytes from normal wild-type mice. Resident intrahepatic NKT ($NK1.1^+$ TCR^+) cells clearly expressed intracellular OPN protein, whereas $NK1.1^-$ conventional T cells did not (Figure 2C). It should be noted that $NK1.1^+TCR^-$ cells, which represent natural killer (NK) cells, also expressed OPN. Since it has been previously shown that depletion of liver NK cells fails to inhibit Con A-induced hepatic injury (Toyabe et al., 1997), we focused on NKT cells as the primary source of OPN. To investigate whether CD1d-restricted classical NKT cells were able to secrete OPN upon activation, we adopted an in vitro system in which $NK1.1^+TCR^+$ NKT cells were stimulated by α-GC in the context of the CD1d molecule. In the presence, but not absence, of α-GC, NKT cells secreted significant amounts of OPN protein, whereas anti-CD3/CD28-stimulated, NKT cell-depleted T cells (i.e., conventional T cells) failed to secrete OPN (Figure 2D). NKT cells also secreted significant amounts of IFN-γ, whereas conventional T cells secreted only a small amount of this cytokine. NKT and conventional T cells secreted similar amounts of TNF-α. To provide further evidence that classical NKT cells are the main source of OPN secretion, we enriched α-GC loaded CD1d-dimer-positive and TCR-positive NKT cells and found that these invariant NKT cells similarly secrete OPN upon stimulation (data not shown). We further tested in vivo production of cytokines and OPN after Con A injection. Liver IFN-γ and TNF-α levels were significantly lower in CD1d- and OPN-deficient mice, as compared with wild-type mice (Figures 2E and 2F). Liver OPN levels were significantly increased after Con A injection in wild-type mice, whereas liver OPN levels remained unchanged in CD1d-deficient mice, in accordance with the plasma OPN levels (Figure 3A). This was confirmed by immunohistochemistry, which showed that liver tissues from wild-type mice indeed express OPN protein after Con A injection (Figure 3B). Collectively, these data indicate that CD1d-restricted classical NKT cells can produce OPN and that these cells are a critical source of plasma OPN in Con A-induced hepatitis.

Role of the Thrombin-Cleaved Form of OPN in Liver Injury

OPN interacts with a variety of cell surface receptors, including αvβ3, αvβ5, α4β1, α8β1, and α9β1 integrins, as well as CD44 (Bayless et al., 1998; Sodek et al., 2000; Yokosaki et al., 1999). Binding of OPN to these cell surface receptors stimulates cell adhesion, migration,

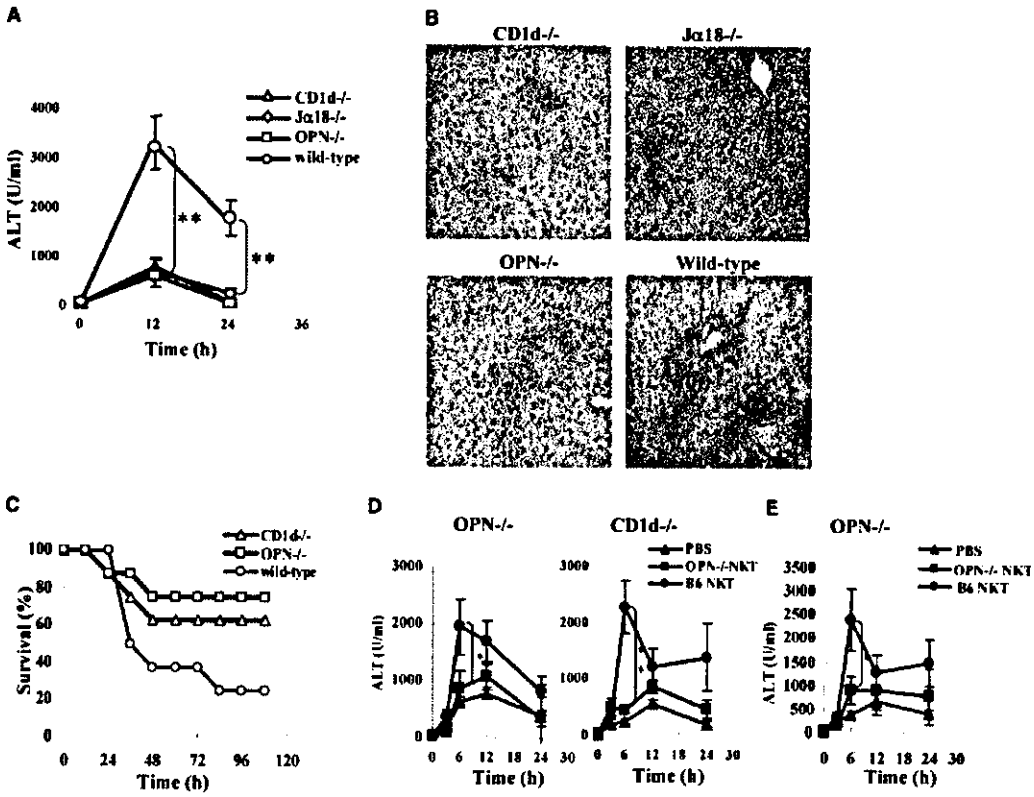

Figure 1. OPN- and NKT Cell-Deficient Mice Fail to Develop Severe Con A-Induced Hepatitis

(A) Serum ALT levels in OPN$^{-/-}$, CD1d$^{-/-}$, Jα18$^{-/-}$, and wild-type mice were assessed after Con A injection. n = 8 per group (Jα18$^{-/-}$; n = 4). **p < 0.001.

(B) Representative liver histology. Livers were obtained at 24 hr after Con A injection, and sections were stained with H&E. Original magnification, 200×.

(C) Survival advantage of OPN$^{-/-}$ and CD1d$^{-/-}$ mice as compared to wild-type mice after 20 mg/kg Con A injection. n = 8 per group.

(D) Restoration of Con A-induced hepatic injury by adoptive transfer of NK1.1^{+}TCR^{+} NKT cells. NKT cells (2×10^6) from wild-type and OPN$^{-/-}$ mice or PBS were injected into recipient OPN$^{-/-}$ and CD1d$^{-/-}$ mice. 1 hr after cell transfer, mice received 10 mg/kg Con A. n = 3 per group. *p < 0.05 and **p < 0.001.

(E) Restoration of Con A-induced hepatic injury by adoptive transfer of α-GC-loaded CD1d dimer^{+}TCR^{+}NKT cells. NKT cells (2×10^6) from wild-type and OPN$^{-/-}$ mice or PBS were injected into recipient OPN$^{-/-}$ mice. 1 hr after cell transfer, mice received 10 mg/kg Con A. n = 3 per group. *, p<0.05 and **, p<0.001.

and specific signaling functions. The major integrin binding domain within OPN is the arginine-glycine-aspartate (RGD) integrin binding motif. However, cleavage of human OPN by thrombin exposes an additional integrin binding motif, the SVVYGLR (SLAYGLR in mice) sequence, which promotes the adherence of cells expressing α4 and α9 integrins. Importantly, this thrombin-cleaved form of OPN has been implicated in the pathogenesis of RA (Yamamoto et al., 2003). Therefore, we examined the molecular nature of OPN in the liver of Con A-injected mice. We found that in addition to the noncleaved form of OPN, a low molecular form of OPN, corresponding to the thrombin-cleaved product, was present in the liver of wild-type mice after Con A injection (Figure 4A). Both noncleaved and cleaved forms of OPN were absent in OPN-deficient mice, even after Con A stimulation (Figure 4A). We then examined the expression of integrins on NKT and conventional T cells. We found that normal intrahepatic NKT cells expressed both α9 and α4 integrins (Figure 4B). In contrast, conventional T cells only expressed α4 integrin. Both NKT and conventional T cells expressed β1 and β3 integrins. We also quantitated integrin expression, which revealed that α9 expression on NKT is twenty times higher than that on conventional T cells, whereas α4 expression on conventional T cells is two times higher than that on NKT cells (Figure 4B). Next, we asked whether the thrombin-cleaved form of OPN, expressed in the liver after Con A injection, plays a role in the development of hepatitis. In vitro migration assays showed that infiltrating leukocytes purified from the liver after Con A injection migrated toward the thrombin-cleaved form of OPN more

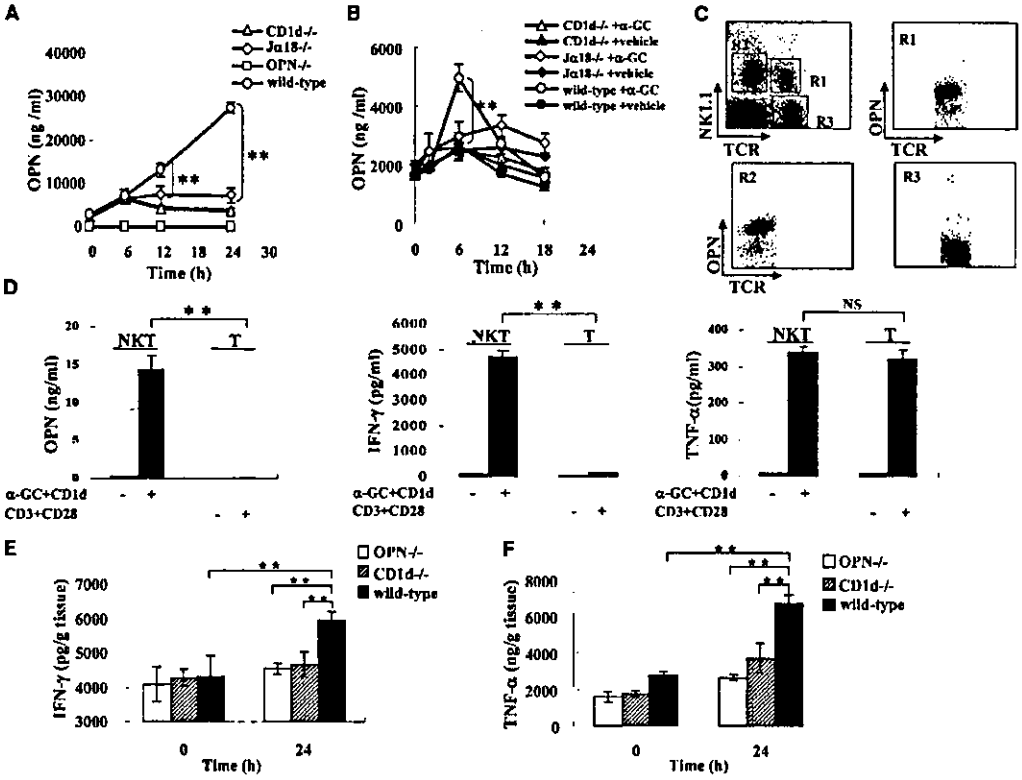

Figure 2. Secretion of OPN and Cytokines Is Defective in NKT Cell-Deficient and OPN$^{-/-}$ Mice

(A and B) Plasma OPN levels in C57BL/6 wild-type, CD1d$^{-/-}$, Jα18$^{-/-}$, and OPN$^{-/-}$ mice were measured by ELISA after Con A (A) or α-GC (B) injection. n = 4 per group. **p < 0.001.

(C) Intracellular OPN expression in intrahepatic leukocytes from wild-type mice. The expression of NK1.1, TCR, and intracellular OPN was analyzed by flow cytometry (upper left). NKT cells as defined by NK1.1$^+$TCR$^+$ (R1) and NK cells as defined by NK1.1$^+$TCR$^-$ (R2) clearly expressed intracellular OPN (upper right and lower left, respectively), whereas conventional T cells as defined by NK1.1$^-$TCR$^+$ (R3) did not (lower right).

(D) Secretion of OPN by NKT cells. NKT and conventional T cells from normal mice were stimulated with α-GC in the presence of CD1d-RBL cells or anti-CD3/CD28 mAbs, respectively, for 3 days. OPN production in the culture supernatant was measured by ELISA. Data are representative of three independent experiments. **p < 0.001.

(E) IFN-γ levels in the liver before and after Con A injection. n = 4 per group. **p < 0.001.

(F) TNF-α levels in the liver before and after Con A injection. n = 4 per group. **p < 0.001.

efficiently than toward the full-length form of OPN (Figure 4C). In sharp contrast, leukocytes obtained from normal livers migrated toward the cleaved form of OPN only marginally. We also examined the type of cells migrating toward the thrombin-cleaved form of OPN by morphological analysis and found that migrating cells were predominantly neutrophils (Figure 4C). We have used antibodies with specificity toward different integrins and specific forms of the OPN molecule to explore the role of OPN cleavage products in Con A-induced hepatic injury. Antibodies directed against β1 and α4 integrins, but not β3 and αv integrins, inhibited the migration of liver-infiltrating cells toward the thrombin-cleaved form of OPN (Figure 4D). Most compellingly, the antibody M5, which was raised against the SLAYGLR peptide (Yamamoto et al., 2003), inhibited cell migration induced by the thrombin-cleaved form of OPN (Figure 4D). The M5 antibody specifically inhibits interaction of this cryptic epitope within the OPN molecule with its receptors, the α4β1 and α9β1 integrins (data not shown). A control anti-OPN antibody M1, raised against the amino-terminal portion of OPN, had no effect on cell migration. Importantly, in vivo M5 antibody treatment significantly reduced serum ALT levels (Figure 4E) and liver necrosis (evaluated by histology) (Figure 4F) in Con A-injected wild-type mice. These data provide strong evidence that the interaction of the thrombin-cleaved form of OPN with its integrin receptor is involved in neutrophil infiltration and liver injury.

OPN Induces Neutrophil Infiltration and Activation during Liver Injury

We then tested whether the absence of OPN or neutralization of OPN by the M5 antibody influences the pro-

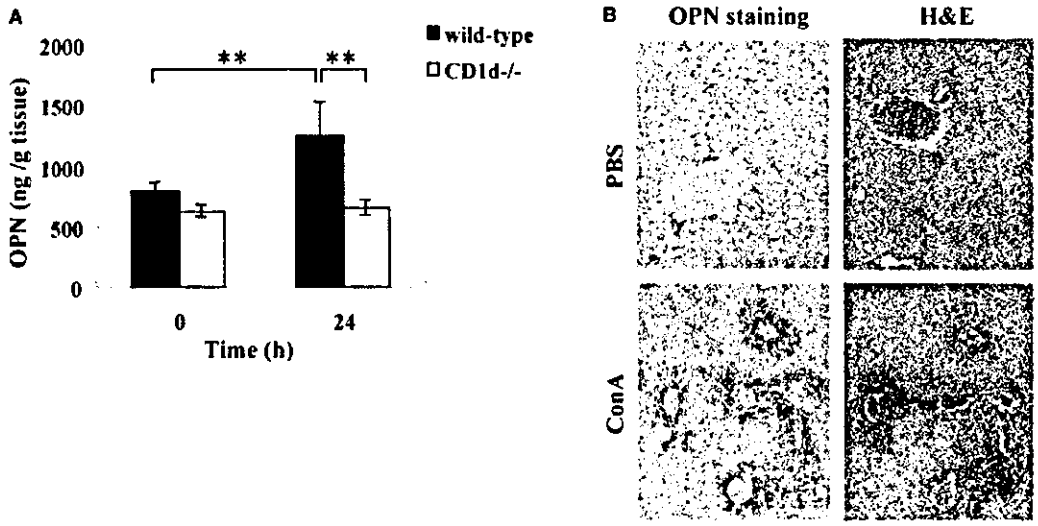

Figure 3. Expression of OPN Protein in the Liver

(A) OPN protein levels in the liver of C57BL/6 wild-type and CD1d-deficient mice after Con A injection. n = 8 per group. **$p < 0.001$.

(B) Immunohistochemical detection of OPN protein in BALB/c mice at 24 hr after PBS (top, left) and Con A (bottom, left) injection. The right panels represent H&E staining of respective sections. Original magnification, 100×. Data are representative of several independent experiments.

duction of a known chemotactic factor for neutrophils, macrophage inflammatory protein-2 (MIP-2) (Feng et al., 1995). We found that intrahepatic NKT cells, but not conventional T cells, from normal wild-type mice expressed MIP-2 (Figure 4B). In wild-type mice serum MIP-2 levels were significantly increased after Con A injection, whereas serum MIP-2 levels were only marginally increased in both OPN- and CD1d-deficient mice (Figure 5A). In addition, in vivo M5 antibody treatment significantly reduced MIP-2 production in the liver in wild-type mice after Con A injection (Figure 5B). These results suggested that OPN might be involved in the regulation of MIP-2 production by NKT cells.

To further address the role of neutrophils in Con A-induced liver injury, we examined the number of liver-infiltrating cells. It should be noted that strong neutrophil infiltration into the liver occurs at 6 hr in Con A-induced hepatitis, preceding the liver tissue damage. In both OPN- and CD1d-deficient mice that were protected from Con A-induced hepatic injury, neutrophil infiltration into the liver was significantly reduced as compared with other cell populations (Figure 6A). At 12 hr, macrophage numbers increased not only in livers from wild-type mice, but also in livers from OPN- and CD1d-deficient mice, indicating that the contribution of macrophages to hepatic injury is not critical. Moreover, neutralization of the thrombin-cleaved form of OPN with the M5 antibody significantly reduced the Con A-induced infiltration of neutrophils, but not that of CD4 T cells or macrophages in wild-type mice (Figure 6B). These results suggested that the thrombin-cleaved form of OPN induces neutrophil infiltration. We also noted that the infiltrating neutrophils expressing myeloperoxidase (MPO) were mainly located in the degenerative area of the liver in Con A-injected wild-type mice (Figure 6C). Interestingly, the amino-terminal half fragment of OPN, which binds to both $\alpha4\beta1$ and $\alpha9\beta1$ integrins (Bayless and Davis, 2001; Smith et al., 1996), efficiently activated neutrophils to secrete MPO. In sharp contrast, both the full-length form of OPN, which binds to $\alpha4\beta1$ (Barry et al., 2000), and the carboxy-terminal fragment of OPN, which binds neither $\alpha4\beta1$ (Barry et al., 2000) nor $\alpha9\beta1$ (Smith et al., 1996), failed to efficiently induce secretion of MPO (Figure 6D). Consistent with these findings, we found that expression of $\alpha9$ and $\alpha4$ integrins was significantly augmented in the liver after Con A injection, but this was substantially reduced after M5 antibody treatment (data not shown). These results indicate that NKT cell-derived OPN contributes to the development of Con A-induced hepatitis through recruitment and activation of neutrophils.

Discussion

NKT cells play a critical role in several models of inflammatory diseases, including multiple sclerosis (MS), rheumatoid arthritis (RA), and atherosclerosis (Chiba et al., 2004; Jahng et al., 2001; Tupin et al., 2004). Interestingly, OPN has also been implicated in the same inflammatory diseases (Chabas et al., 2001; Matsui et al., 2003; Ohshima et al., 2002; Steinman and Zamvil, 2003; Yumoto et al., 2002). However, until now, it has remained unclear whether there is any mechanistic link between OPN and NKT cells for the development of inflammatory diseases. To search for a possible link between OPN and NKT cells in inflammatory disease, we used Con A-induced fulminant hepatitis, a well-characterized murine model of inflammatory liver disease. We found that both NKT- and OPN-deficient mice are resistant to Con A-induced hepatic injury. More importantly, we demonstrated that adoptive

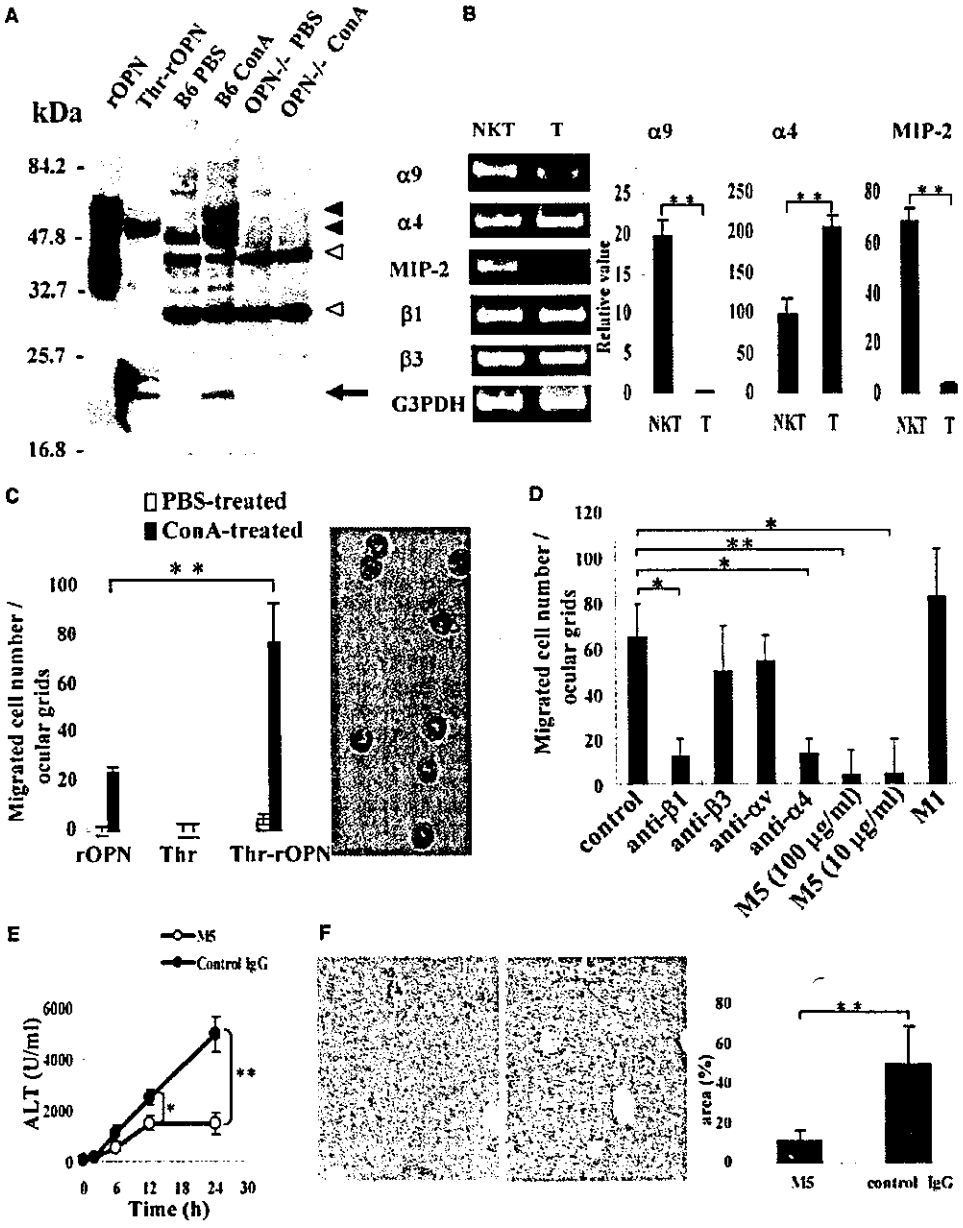

Figure 4. Critical Involvement of the Thrombin-Cleaved Form of OPN in Con A-Induced Hepatitis

(A) Western blot analysis of liver extracts. Liver extracts were prepared from wild-type and OPN$^{-/-}$ mice 24 hr after PBS or Con A injection. Recombinant OPN (rOPN) and thrombin-treated rOPN (Thr-rOPN) were used as controls. A low molecular form of OPN is indicated by the arrow. Closed arrowheads indicate the full-length OPN and open arrowheads indicate nonspecific bands.

(B) RT-PCR (left) and quantitative real time PCR (right) analyses of gene expression of integrins and MIP-2 in NKT and conventional T cells of normal C57BL/6 mice. In quantitative real-time PCR analyses, the relative value of gene expression was normalized against the gene expression levels of G3PDH. Data are representative of three independent experiments.

(C) Migration of liver-infiltrating leukocytes toward the thrombin-cleaved form of OPN. Infiltrating leukocytes prepared from the liver of BALB/c mice 6 hr after Con A or PBS injection were tested for their migratory activity against 10 μg/ml of full-length OPN (rOPN), 1 U/ml of thrombin (Thr), or 10 μg/ml of thrombin-treated rOPN (Thr-rOPN). Background cell migration toward medium only was subtracted. Migrated cells were recovered and stained with Diff-Quik. Original magnification, 400×. Data are representative of three independent experiments.

(D) Migration assays were performed in the presence of various antibodies. Antibody concentrations used were 100 μg/ml unless specifically

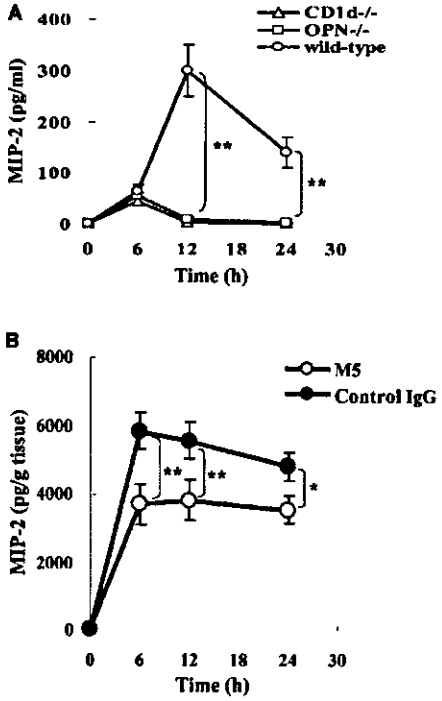

Figure 5. The Absence of OPN or Neutralization of OPN by M5 Antibody Influence the Production of MIP-2

(A) MIP-2 protein levels in the serum of $OPN^{-/-}$, $CD1d^{-/-}$, and wild-type mice after Con A injection. n = 4 per group. $^{**}p < 0.001$.

(B) Inhibitory effect of M5 antibody on liver MIP-2 levels. n = 6 per group. $^{*}p < 0.05$ and $^{**}p < 0.001$.

transfer of $NK1.1^+TCR^+$NKT cells from wild-type, but not OPN-deficient, mice restores Con A-induced hepatic injury in both OPN- and CD1d-deficient mice. We also found that normal intrahepatic NKT cells express OPN and that purified NKT cells secrete substantial amounts of OPN upon activation. Consequently, OPN levels were significantly increased after Con A injection in wild-type mice, but remained unchanged in CD1d-deficient mice. Consistent with those findings, plasma OPN levels were very low after Con A injection in CD1d- and Jα18-deficient mice. Thus NKT cells are an important cellular source of plasma OPN after Con A injection. In addition, we found that plasma OPN levels are significantly elevated after treatment of wild-type mice with α-GC, a potent NKT cell activator, whereas plasma levels in OPN- and CD1d-deficient mice were not significantly increased. These findings demonstrate a critical link between OPN and NKT cells in the pathogenesis of Con A-induced hepatitis.

We noted that Con A administration resulted in a progressive increase and high levels of plasma OPN, whereas α-GC induced only transient and low levels of OPN in wild-type mice. A likely explanation for these findings is that Con A stimulates not only secretion of stored OPN but also de novo synthesis of OPN, whereas α-GC only stimulates secretion of stored OPN. An alternative possibility is that Con A remains in the liver for an extended timeperiod, therefore stimulating NKT cells chronically, whereas the half-life of α-GC in the blood is relatively short. In addition, we showed that hepatic resident NK cells as defined by $NK1.1^+TCR^-$ expressed OPN. Thus it is possible that in addition to NKT cells, hepatic NK cells also contribute to the production of OPN in Con A-induced hepatitis. However, deletion of NK cells did not inhibit the development of Con A-induced hepatic injury (Toyabe et al., 1997), indicating that NK cell involvement in Con A-induced hepatic injury is not critical. In the case of IFN-γ production in response to α-GC treatment of mice, the initial burst of IFN-γ was derived from NKT cells, which stimulated IFN-γ production by NK cells, thus contributing to sustained serum IFN-γ levels (Smyth et al., 2002). In contrast, α-GC induced only a sharp and transient, but not sustained, OPN production, indicating that NK cells are not involved in α-GC-induced OPN production. We also found that hepatic NKT cells expressed both OPN and its receptors, α9 and α4 integrins. Importantly, liver tissues expressed both the noncleaved and thrombin-cleaved forms of OPN after Con A injection. We demonstrated that the thrombin-cleaved form of OPN was critically involved in the pathogenesis of Con A-induced liver injury since the M5 antibody that specifically recognizes the cryptic epitope exposed by thrombin digestion and interferes with the binding of a cryptic epitope to α9β1 and α4β1 integrins inhibited Con A-induced hepatic injury. In this regard, it has been shown that the ratio of the thrombin-cleaved form of OPN to the noncleaved form was significantly increased in the plasma and synovial fluid of RA patients compared with plasma from healthy control and osteoarthritic patients (Ohshima et al., 2002). Nevertheless, M5 antibody treatment also resulted in amelioration of disease in a murine model of RA (Yamamoto et al., 2003).

Our findings support a recent study showing the importance of thrombin in Con A-induced hepatic injury. Inhibition of thrombin activity by antithrombin III significantly attenuated the degree of liver injury as indicated by ALT levels and neutrophil infiltration (Nakamura et al., 2002). However, thrombin is generated during tissue damage in various organs, including the liver (Esmon,

indicated. Data are representative of three independent experiments. Background cell migration toward medium only was subtracted. $^{*}p < 0.05$ and $^{**}p < 0.001$.

(E) Effect of M5 antibody on serum ALT levels in BALB/c mice after Con A injection. Mice were treated with M5 antibody or control IgG. $^{*}p < 0.05$ and $^{**}p < 0.001$. The discrepancy in the levels of ALT between Figures 1 and 4 was due to the strain difference; B6 mice were used in Figure 1 and BALB/c mice in Figure 4.

(F) Representative liver histology of BALB/c mice treated with M5 antibody or control IgG. Livers were obtained at 24 hr after Con A injection and liver sections were stained with H&E. Original magnification, 100×. Degenerative area per liver section was quantitated by using NIH image 1.62. $^{**}p < 0.001$.

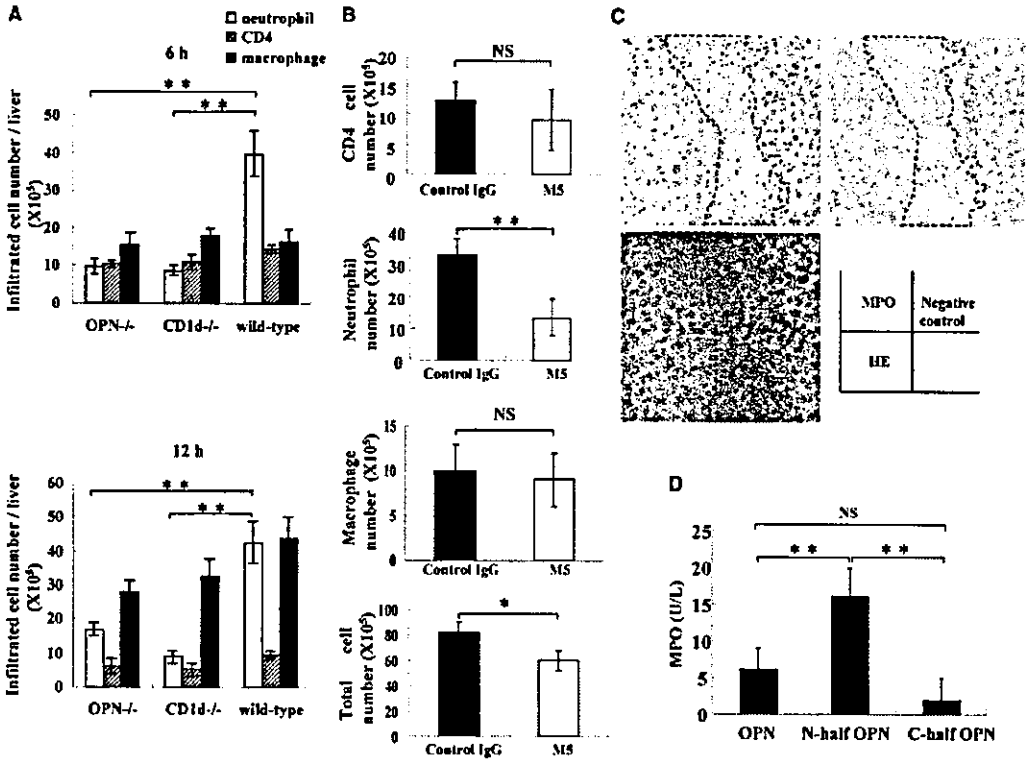

Figure 6. The Predominant Liver-Infiltrating Leukocytes in Con A-Induced Hepatitis Are Neutrophils

(A) Liver-infiltrating leukocytes were prepared from C57BL/6 wild-type, CD1d$^{-/-}$, and OPN$^{-/-}$ mice at 6 and 12 hr after Con A injection. The number of Gr1$^+$ CD11b$^+$ neutrophils, CD4$^+$ T cells, and F4/80$^+$ macrophages was determined by flow cytometry. n = 3 per group. $^{**}p < 0.001$.

(B) Effect of M5 antibody on infiltration of neutrophils. Con A-injected mice were treated with control IgG or M5 antibody. At 6 hr, liver-infiltrating leukocytes were analyzed for CD4$^+$ T cells, Gr1$^+$CD11b$^+$ neutrophils, and F4/80$^+$ macrophage number by flow cytometry. n = 3 per group. $^{**}p < 0.001$.

(C) Immunohistochemical detection of neutrophils. Livers were obtained from BALB/c mice at 24 hr after Con A injection, and sections were stained with anti-MPO or H&E. Sections were also stained with secondary antibody only as a negative control. Dotted lines indicate the area of liver degeneration. Original magnification, 200×.

(D) OPN-induced production of MPO. Neutrophils obtained from BALB/c mice were stimulated with 20 μg/ml of GST fusion proteins containing full-length OPN (OPN), N-terminal half of OPN (N-half OPN), or C-terminal half of OPN (C-half OPN) for 36 hr. Background production of MPO by neutrophils stimulated with GST was subtracted. Data are representative of three independent experiments. $^{**}p < 0.001$.

1993). Nevertheless, thrombin could contribute to Con A-induced hepatic injury in many other ways. For example, thrombin may activate coagulation to increase hepatic sinusoidal hemostasis, which in turn results in liver tissue injury (Arai et al., 1996). Alternatively, thrombin may induce expression of IL-8 and leukocyte adhesion molecules including P-selectin, E-selectin, and ICAM-1 on endothelial cells (Leirisalo-Repo, 1994), promoting leukocyte activation (Copple et al., 2003). However, we favor the interpretation that at the earliest stage of Con A-induced hepatitis, activated NKT cells secrete OPN, which is subsequently cleaved by thrombin to expose the cryptic OPN epitope SLAYGLR, thereby activating receptors for this epitope, such as the $\alpha 9\beta 1$ and $\alpha 4\beta 1$ integrins expressed by NKT cells. This interaction of OPN with its receptor could further activate NKT cells and contribute to liver cell injury in Con A-induced hepatitis.

We found that strong cellular infiltration into the liver occurred at an early stage of Con A-induced hepatitis, preceding the liver tissue damage. We further showed that among these infiltrating cells, neutrophils were abundant. The appearance of neutrophils in Con A-induced hepatitis was demonstrated in several previous studies (Bajt et al., 2001; Jaruga et al., 2003; Miyazawa et al., 1998). Our data strongly indicate that neutrophils play a pivotal role in liver injury after Con A injection. The distribution of neutrophils in the liver, as defined by MPO activity, correlated well with the area of liver degeneration. Hydrogen peroxide, produced by activated neutrophils, is transformed by MPO into an array of potentially damaging reactants and causes acute liver injury (Brown et al., 2001). In both OPN- and CD1d-deficient mice that were protected from Con A-induced hepatic injury, neutrophil infiltration into the liver was significantly reduced as compared to other cell populations. Importantly, it has been shown that depletion of neutrophils by anti-Gr1 antibody prevents the development of hepatitis

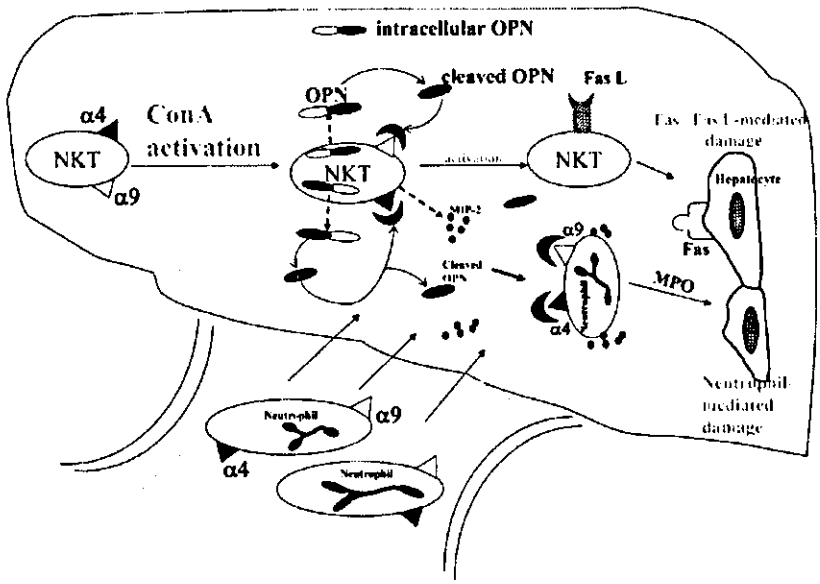

Figure 7. Schematic Representation of the Link between OPN, NKT Cells, and Neutrophils in Con A-Induced Hepatic Injury

Intrahepatic resident NKT cells express α9 and α4 integrins, receptors for the thrombin-cleaved form of OPN. After Con A-induced activation, NKT cells secrete OPN, which is presumably cleaved by thrombin in the liver. The interaction of NKT cells and the thrombin-cleaved form of OPN through its receptors further activates NKT cells. MIP-2, a known chemotactic factor, is produced in the liver upon Con A stimulation. Activated NKT cells express FasL and contribute to Fas/FasL-mediated liver cell injury. On the other hand, the thrombin-cleaved form of OPN, together with MIP-2, recruits neutrophils into the liver. Upon interaction of the thrombin-cleaved form of OPN with its receptors on neutrophils, the latter cells become activated, secrete MPO, and contribute to additional liver cell damage.

and reduces the liver damage in Con A-induced hepatitis (Bonder et al., 2004). Therefore, we explored how OPN regulates neutrophil function. We demonstrated that the amino-terminal half of OPN, which contains the cryptic epitope SLAYGLR, could activate neutrophils to release MPO. We also found that the thrombin-cleaved form of OPN can induce migration of neutrophils in vitro. The M5 antibody, as well as anti-β1 and anti-α4 integrin mAbs, was able to inhibit this cell migration. Furthermore, the infiltration of neutrophils into the liver was significantly inhibited by the M5 antibody treatment. Neutrophils are known to express the α9β1 integrin and, to a lesser extent, the α4β1 integrin, and lymphocytes do not express the α9β1 integrin (Bayless et al., 1998; Yokasaki and Sheppard, 2000). Thus, it is possible that neutrophils, through interaction of both α9β1 and α4β1 with the thrombin-cleaved form of OPN, are involved in neutrophil infiltration and activation, leading to liver damage. Consistent with our data, it was previously shown that blocking either the α4 or α9 integrin by antibodies inhibited neutrophil transendothelial migration (Taooka et al., 1999).

We also found that Con A induced, in an NKT cell-dependent manner, production of MIP-2, which is chemotactic for neutrophils. However, we were unable to detect significant levels of MIP-2 production by purified NKT cells after Con A stimulation in vitro (data not shown). This may indicate that there is crosstalk between NKT and other cell types that produce MIP-2 in response to NKT cell activation, as has been described for other cytokines (Kitamura et al., 1999; Smyth et al., 2002). It is tempting to speculate that initial activation of NKT cells by Con A may lead to MIP-2 production by dendritic cells. In this regard, it has been known that MIP-2 not only recruits neutrophils but also NKT cells (Faunce et al., 2001). In addition, OPN recruits dendritic cells (Tanaka et al., 2004). Importantly, MIP-2 levels in the liver were upregulated by Con A injection, which was significantly inhibited by M5 antibody. Thus, in addition to the thrombin-cleaved form of OPN, MIP-2 may also contribute to the infiltration of neutrophils into the liver and the subsequent liver injury.

In conclusion, during the course of Con A-induced hepatitis, activated NKT cells secrete OPN, which also leads to production of MIP-2, two cytokines that are chemotactic for neutrophils. We propose that the interaction of a cryptic epitope of OPN, SLAYGLR with the α9β1 and α4β1 integrins on NKT cells, and neutrophils contributes to the hepatic injury induced by Con A as illustrated in Figure 7. Targeting this OPN epitope could represent a new modality for the treatment of inflammatory hepatitis. A similar mechanism may also contribute to the development of other inflammatory diseases in which NKT cells and OPN have been implicated.

Experimental Procedures

Animals

Specific pathogen-free female BALB/c and C57BL/6 (B6) (6-week-old) mice were purchased from Japan SLC (Shizuoka, Japan). OPN-deficient ($OPN^{-/-}$) mice (Rittling et al., 1998) backcrossed 11 times to B6 mice at the Institute for Genetic Medicine, Hokkaido University were used. CD1d-deficient ($CD1d^{-/-}$) and Jα18-deficient

($J\alpha18^{-/-}$) mice of B6 origin were generated as described (Cui et al., 1997; Singh et al., 1999). All mice were maintained under specific pathogen-free conditions and used according to the institutional guidelines.

Antibodies

Antibodies used for blocking studies were as follows: polyclonal M5 antibody that specifically recognizes SLAYGLR (Yamamoto et al., 2003), polyclonal M1 antibody that specifically recognizes the amino-terminal portion of murine OPN (Yamamoto et al., 2003), and monoclonal antibodies (mAbs) directed against β1 integrin (HMβ1) (Noto et al., 1995) and β3 integrin (HMβ3) (Yasuda et al., 1995). Anti-αv integrin (RMV-7) and anti-α4 integrin (R1-2) were purchased from PharMingen (San Diego, CA). Antibodies for FACS staining were anti-CD4-PE (L3T4), anti-CD11b-PE (M1/70), anti-Gr1-FITC (RB6-8C5), anti-NK1.1-PE(PK136), anti-TCRβ-FITC (H57-597) and streptavidin-APC (all from PharMingen, San Diego, CA), biotin-anti-F4/80 (A3-1) (Caltag Laboratories, Burlingame, CA), and biotin-anti-OPN (O-17) (IBL, Gunma, Japan). Antibodies for immunohistochemistry were biotin-anti-CD4 (L3T4), biotin-anti-Gr-1 (RB6-8C5) (all from PharMingen, San Diego, CA), and polyclonal rabbit anti-mouse OPN antibody (O-17) (IBL, Gunma, Japan).

Con A-Induced Hepatitis

Mice were injected intravenously through the tail vein with Con A (Vector Laboratories, Burlingame, CA) reconstituted in pyrogen-free PBS. In general, the dose of Con A was 15 mg/kg and 10 mg/kg for BALB/c mice and mice of the C57BL/6 background, respectively. For survival studies, mice were injected with 20 mg/kg of Con A. For the indicated experiments, 400 μg of M5 Ab or normal rabbit IgG was dissolved in 200 μl of PBS. These antibodies were administered to mice intravenously 3 hr before Con A challenge. Serum alanine aminotransferase (ALT) levels were measured by using a standard clinical automatic analyzer.

Preparation of Liver-Infiltrating Leukocytes

Liver-infiltrating leukocytes were isolated as previously described (Takahashi et al., 2001). Briefly, livers were minced, pressed through a stainless steel mesh, and suspended in PBS. After washing, the cells were resuspended in 33% Percoll solution containing heparin (100 U/ml) and centrifuged at 2000 rpm for 15 min to remove liver parenchymal cells. The pellet was treated with an RBC lysis solution, washed with PBS three times, and then resuspended in 10% FCS-DMEM.

In Vitro Migration Assay

In vitro migration assay was performed by using a 24-well Transwell tissue culture plate (Costar, Corning, NY) with polycarbonate filter (pore size, 5 μm). Recombinant murine OPN (IBL, Gunma, Japan) digested by thrombin at 10 μg of OPN per 1 U of enzyme at 37°C for 1 hr was used as a chemoattractant. In some experiments, the cells were incubated with the indicated antibodies at a concentration of 100 μg/ml at 37°C for 15 min. After incubation at 37°C for 2 hr, the migrated cell numbers were quantitated by cell counts of 100 fields by using 100 ocular grids (×100). Migrated cells were recovered and stained with Diff-Quik (International Reagents Corporation, Kobe, Japan).

Morphometric Analysis

Formalin-fixed and paraffin-embedded sections were stained with hematoxylin and eosin (H&E). Necrotic areas were measured in each section by using NIH image 1.62 followed by calculation of the necrotic area per section.

Immunohistochemistry

The expression of OPN was assessed by using polyclonal rabbit anti-mouse OPN antibody. Sections of paraffin-embedded liver tissue were processed for immunohistochemistry as previously described (Yoneyama et al., 1998). Immunohistochemical detection of MPO was performed by using a rabbit anti-human MPO Ab (DAKO, Carpinteria, CA) that crossreacts with mouse MPO (Grone et al., 2002).

Flow Cytometry

Liver-infiltrating leukocytes were stained with anti-CD4, anti-Gr1, and anti-CD11b mAbs as previously described (Moriyama et al., 1997). For intracellular OPN staining, leukocytes obtained from the liver were cultured in the presence of 2 μM monensin for 90 min and then stained by surface markers with anti-NK1.1 and anti-TCRβ. Cells were then fixed with 4% paraformaldehyde for 10 min and permeablized with a solution of 1% FCS, 0.1% saponin, and 0.1% sodium azide in PBS. Intracellular staining was performed using biotin-anti-OPN at 3 μg/ml diluted in 0.1% saponin staining buffer and Streptavidin-APC was used as the secondary reagent. All analyses were performed on a FACSCalibur (BD, Mountain View, CA) with CellQuest software.

In Vitro and In Vivo NKT and Conventional T Cell Stimulation

NKT and conventional T cells were isolated by a combination of magnetic-activated cell sorting (MACS) and FACS as previously described (Iwabuchi et al., 2001). In brief, $CD24^{-}CD8^{-}$ cells were negatively selected by using anti-CD24 and anti-CD8 magnetic beads. The $CD24^{-}CD8^{-}$ cells were stained with FITC-anti-TCR mAb and PE-anti-NK1.1 mAb and sorted into $NK1.1^{+}TCR^{+}$ (NKT) cells and $NK1.1^{-}TCR^{+}$ (conventional T) cells with a FACS Vantage instrument (Becton Dickinson). The sorted NKT cells and conventional T cells were cultured overnight with recombinant IL-2. NKT cells were further stimulated with 100 ng/ml α-GC in the presence of 100Gy-irradiated rat basophilic leukemia (RBL) cells transfected with CD1d. T cells were stimulated with anti-CD3 (145-2C11) and anti-CD28 (37.51) mAbs. In some experiments, mice were intravenously injected with 100 μg/kg α-GC or vehicle. α-GC was kindly provided by the Institute of Pharmaceutical Research, Kirin Brewery Co. (Gunma, Japan). CD1d-transfected cells were provided by Dr. Albert Bendelac (University of Chicago, Chicago, IL).

Adoptive Transfer of NKT Cells

Intrahepatic leukocytes were stained with PE-anti-NK1.1 and FITC-anti-TCRβ mAb. Cells were also stained with α-GC-loaded CD1d-dimer (BD Biosciences PharMingen) according to the method provided by the manufacturer followed by staining with FITC-anti-TCRβ. Cells were then sorted into $NK1.1^{+}TCR^{+}$ or $CD1d\text{-}dimer^{+}TCR^{+}$ cells. These cells, in a volume of 50 μl, were injected into the liver of recipient mice (2×10^{6} cells/mouse) 1 hr before Con A challenge (10 mg/kg). Sera were obtained from individual mice at the time point indicated in the figures, and serum ALT levels were determined.

Tissue Extraction, SDS-PAGE, and Western Blot Analysis

For Western blot analysis, mouse tissues were pulverized in PBS containing protease inhibitor cocktail (Roche, Mannheim, Germany). Further homogenization was done by repeated sonication for 15 s. After calibration of protein content, 15 μg each of protein extract was electrophoresed through 10 to 20% polyacrylamide Tris HCl Ready Gels (BioRad Laboratories, Hercules, California) and probed with polyclonal anti-OPN antibody (IBL, Gunma, Japan) as described previously (Kon et al., 2002).

ELISA

OPN, MIP-2 (both from IBL, Gunma, Japan) and TNF-α and IFN-γ (both from PharMingen, San Diego, CA) concentration were measured by using ELISA kits as specified by the manufacturers. Cytokine contents in the liver extracts were expressed as amounts per 1 g of liver tissue. MPO production was measured as described (Ramsaransing et al., 2003).

Analysis of mRNA Expression

Total RNA was isolated by using Trizol (Life Technologies, Gaithersburg, MD). The specific primers used were as follows. Glyceraldehyde-3-phosphate dehydrogenase (G3PDH): 5′-ACCACAGTCCATGCCATCAC-3′ (sense), 5′-TCCACCACCCCTGTTGCTGTA-3′ (antisense). α4 integrin: 5′-TGGAAGCTACTTAGGCTACT-3′ (sense), 5′-TCCCACGACTTCGGTAGTAT-3′ (antisense). α9 integrin, 5′-AAAGGCTGCAGCTGTCCCACATGGACGAAG-3′ (sense), 5′-TTTAGAGAGATATTCTTCACAGCCCCCAAA-3′ (antisense). MIP-2: 5′-GAACAAAGGCAAGGCTAACTGA-3′ (sense), 5′-AACATAACAACATCTGGGCAAT-3′ (antisense). β1 integrin: 5′-CAAGGAGAAGGACATTGAT

GAC-3′ (sense), 5′-TCATTTTCCCTCATACTTCGG-3′ (antisense). β3 integrin: 5′-TTCGACTACGGCCAGATGATTC-3′ (sense), 5′-TTTCT CAGTCATCAGCCCCAG-3′ (antisense). Quantitative real-time PCR analysis of mRNA expression was also carried out with LightCycler Fast Start DNA Master SYBR Green I Systems (Roche Diagnostics). The expression of mRNA was calculated by LightCycler Software, version 3. Data were standardized by G3PDH.

Construction of the GST-OPN Fusion Plasmid and Protein Purification

OPN is specifically cleaved by thrombin between R154 and S155, thus making amino-terminal and carboxy-terminal fragments of OPN. Full-length (L17–N294), amino-terminal fragments (N-half OPN) (L17–R154), and carboxy-terminal fragments (C-half OPN) (S155–N294) of murine OPN cDNA were amplified from the first strand cDNA obtained from mouse kidney by using the following primers: Full-length OPN, 5′-TAGGGATCCCTCCCGGTGAAAGTGA CTGAT-3′ (sense) and 5′-GTCTCGAGTTAGTTGACCTCAGAAGA TGA-3′ (antisense); N-half OPN, full-length OPN sense primer and 5′-AACCTCGAGTTACCTCAGTCCATAAGCCAA-3′ (antisense); C-half OPN, 5′-CAGGGATCCTCAAAGTCTAGGAGTTTCCAG-3′ (sense) and full-length OPN antisense primer. PCR products were digested with BamHI and XhoI, ligated into pGEX6P-1 (Amersham Bioscience, Piscataway, NJ), and sequenced. The recombinant GST-OPN fusion proteins were prepared in *E. coli* as described previously (Kon et al., 2002). The GST fusion proteins were purified on glutathione-Sepharose columns as described (Tanaka et al., 2004).

Statistics

Data are presented as means ± SEM and are representative of at least two independent in vitro experiments. The significance of differences between two groups was determined by using a Student's t test. $^{*}p < 0.05$. $^{**}p < 0.001$. NS, not significant.

Acknowledgments

We are grateful to Dr. Dean Sheppard (UCSF) for his critical comments and for reviewing the manuscript. This study was supported by grants from the Ministry of Education, Culture, Sports, Science, and Technology and the Ministry of Health, Labor and Welfare of Japan.

Received: April 1, 2004
Revised: July 19, 2004
Accepted: August 18, 2004
Published: October 19, 2004

References

Arai, M., Mochida, S., Ohno, A., and Fujiwara, K. (1996). Blood coagulation in the hepatic sinusoids as a contributing factor in liver injury following orthotopic liver transplantation in the rat. Transplantation *62*, 1398–1401.

Ashkar, S., Weber, G.F., Panoutsakopoulou, V., Sanchirico, M.E., Jansson, M., Zawaideh, S., Rittling, S.R., Denhardt, D.T., Glimcher, M.J., and Cantor, H. (2000). Eta-1 (osteopontin): an early component of type-1 (cell-mediated) immunity. Science *287*, 860–864.

Bajt, M.L., Farhood, A., and Jaeschke, H. (2001). Effects of CXC chemokines on neutrophil activation and sequestration in hepatic vasculature. Am. J. Physiol. Gastrointest. Liver Physiol. *281*, G1188–G1195.

Barry, S.T., Ludbrook, S.B., Murrison, E., and Horgan, C.M. (2000). Analysis of the alpha4beta1 integrin-osteopontin interaction. Exp. Cell Res. *258*, 342–351.

Bayless, K.J., and Davis, G.E. (2001). Identification of dual alpha 4beta1 integrin binding sites within a 38 amino acid domain in the N-terminal thrombin fragment of human osteopontin. J. Biol. Chem. *276*, 13483–13489.

Bayless, K.J., Meininger, G.A., Scholtz, J.M., and Davis, G.E. (1998). Osteopontin is a ligand for the alpha4beta1 integrin. J. Cell Sci. *111*, 1165–1174.

Bonder, C.S., Ajuebor, M.N., Zbytnuik, L.D., Kubes, P., and Swain, M.G. (2004). Essential role for neutrophil recruitment to the liver in concanavalin A-induced hepatitis. J. Immunol. *172*, 45–53.

Brown, K.E., Brunt, E.M., and Heinecke, J.W. (2001). Immunohistochemical detection of myeloperoxidase and its oxidation products in Kupffer cells of human liver. Am. J. Pathol. *159*, 2081–2088.

Burdin, N., Brossay, L., Koezuka, Y., Smiley, S.T., Grusby, M.J., Gui, M., Taniguchi, M., Hayakawa, K., and Kronenberg, M. (1998). Selective ability of mouse CD1 to present glycolipids: alpha-galactosylceramide specifically stimulates V alpha 14+ NK T lymphocytes. J. Immunol. *161*, 3271–3281.

Chabas, D., Baranzini, S.E., Mitchell, D., Bernard, C.C., Rittling, S.R., Denhardt, D.T., Sobel, R.A., Lock, C., Karpuj, M., Pedotti, R., et al. (2001). The influence of the proinflammatory cytokine, osteopontin, on autoimmune demyelinating disease. Science *294*, 1731–1735.

Chen, D., McKallip, R.J., Zeytun, A., Do, Y., Lombard, C., Robertson, J.L., Mak, T.W., Nagarkatti, P.S., and Nagarkatti, M. (2001). CD44-deficient mice exhibit enhanced hepatitis after concanavalin A injection: evidence for involvement of CD44 in activation-induced cell death. J. Immunol. *166*, 5889–5897.

Chiba, A., Oki, S., Miyamoto, K., Hashimoto, H., Yamamura, T., and Miyake, S. (2004). Suppression of collagen-induced arthritis by natural killer T cell activation with OCH, a sphingosine-truncated analog of alpha-galactosylceramide. Arthritis Rheum. *50*, 305–313.

Copple, B.L., Moulin, F., Hanumegowda, U.M., Ganey, P.E., and Roth, R.A. (2003). Thrombin and protease-activated receptor-1 agonists promote lipopolysaccharide-induced hepatocellular injury in perfused livers. J. Pharmacol. Exp. Ther. *305*, 417–425.

Cui, J., Shin, T., Kawano, T., Sato, H., Kondo, E., Toura, I., Kaneko, Y., Koseki, H., Kanno, M., and Taniguchi, M. (1997). Requirement for Valpha14 NKT cells in IL-12-mediated rejection of tumors. Science *278*, 1623–1626.

Diao, J., Garces, R., and Richardson, C.D. (2001). X protein of hepatitis B virus modulates cytokine and growth factor related signal transduction pathways during the course of viral infections and hepatocarcinogenesis. Cytokine Growth Factor Rev. *12*, 189–205.

Esmon, C.T. (1993). Cell mediated events that control blood coagulation and vascular injury. Annu. Rev. Cell Biol. *9*, 1–26.

Faunce, D.E., Sonoda, K.H., and Stein-Streilein, J. (2001). MIP-2 recruits NKT cells to the spleen during tolerance induction. J. Immunol. *166*, 313–321.

Feng, L., Xia, Y., Yoshimura, T., and Wilson, C.B. (1995). Modulation of neutrophil influx in glomerulonephritis in the rat with anti-macrophage inflammatory protein-2 (MIP-2) antibody. J. Clin. Invest. *95*, 1009–1017.

Grone, H.J., Grone, E.F., and Malle, E. (2002). Immunohistochemical detection of hypochlorite-modified proteins in glomeruli of human membranous glomerulonephritis. Lab. Invest. *82*, 5–14.

Iwabuchi, K., Iwabuchi, C., Tone, S., Itoh, D., Tosa, N., Negishi, I., Ogasawara, K., Uede, T., and Onóe, K. (2001). Defective development of NK1.1+ T-cell antigen receptor alphabeta+ cells in zeta-associated protein 70 null mice with an accumulation of NK1.1+ CD3- NK-like cells in the thymus. Blood *97*, 1765–1775.

Jahng, A.W., Maricic, I., Pedersen, B., Burdin, N., Naidenko, O., Kronenberg, M., Koezuka, Y., and Kumar, V. (2001). Activation of natural killer T cells potentiates or prevents experimental autoimmune encephalomyelitis. J. Exp. Med. *194*, 1789–1799.

Jaruga, B., Hong, F., Sun, R., Radaeva, S., and Gao, B. (2003). Crucial role of IL-4/STAT6 in T cell-mediated hepatitis: up-regulating eotaxins and IL-5 and recruiting leukocytes. J. Immunol. *171*, 3233–3244.

Kaneko, Y., Harada, M., Kawano, T., Yamashita, M., Shibata, Y., Gejyo, F., Nakayama, T., and Taniguchi, M. (2000). Augmentation of Valpha14 NKT cell-mediated cytotoxicity by interleukin 4 in an autocrine mechanism resulting in the development of concanavalin A-induced hepatitis. J. Exp. Med. *191*, 105–114.

Kawano, T., Cui, J., Koezuka, Y., Toura, I., Kaneko, Y., Motoki, K., Ueno, H., Nakagawa, R., Sato, H., Kondo, E., et al. (1997). CD1d-restricted and TCR-mediated activation of Valpha14 NKT cells by glycosylceramides. Science *278*, 1626–1629.

Kitamura, H., Iwakabe, K., Yahata, T., Nishimura, S., Ohta, A., Ohmi, Y., Sato, M., Takeda, K., Okumura, K., Van Kaer, L., et al. (1999). The natural killer T (NKT) cell ligand alpha-galactosylceramide demonstrates its immunopotentiating effect by inducing interleukin (IL)-12 production by dendritic cells and IL-12 receptor expression on NKT cells. J. Exp. Med. *189*, 1121–1128.

Kon, S., Yokosaki, Y., Maeda, M., Segawa, T., Horikoshi, Y., Tsukagoshi, H., Rashid, M.M., Morimoto, J., Inobe, M., Shijubo, N., et al. (2002). Mapping of functional epitopes of osteopontin by monoclonal antibodies raised against defined internal sequences. J. Cell. Biochem. *84*, 420–432.

Leirisalo-Repo, M. (1994). The present knowledge of the inflammatory process and the inflammatory mediators. Pharmacol. Toxicol. Suppl. *75*, 1–3.

Louis, H., Le Moine, O., Peny, M.O., Quertinmont, E., Fokan, D., Goldman, M., and Deviere, J. (1997). Production and role of interleukin-10 in concanavalin A-induced hepatitis in mice. Hepatology *25*, 1382–1389.

Matsui, Y., Rittling, S.R., Okamoto, H., Inobe, M., Jia, N., Shimizu, T., Akino, M., Sugawara, T., Morimoto, J., Kimura, C., et al. (2003). Osteopontin deficiency attenuates atherosclerosis in female apolipoprotein E-deficient mice. Arterioscler. Thromb. Vasc. Biol. *23*, 1029–1034.

McFarlane, I.G. (1999). Pathogenesis of autoimmune hepatitis. Biomed. Pharmacother. *53*, 255–263.

Miyazawa, Y., Tsutsui, H., Mizuhara, H., Fujiwara, H., and Kaneda, K. (1998). Involvement of intrasinusoidal hemostasis in the development of concanavalin A-induced hepatic injury in mice. Hepatology *27*, 497–506.

Morimoto, J., Inobe, M., Kimura, C., Kon, S., Diao, H., Aoki, M., Miyazaki, T., Denhardt, D.T., Rittling, S., and Uede, T. (2004). Osteopontin affects the persistence of beta-glucan-induced hepatic granuloma formation and tissue injury through two distinct mechanisms. Int. Immunol. *16*, 477–488.

Moriyama, H., Yamamoto, T., Takatsuka, H., Umezu, H., Tokunaga, K., Nagano, T., Arakawa, M., and Naito, M. (1997). Expression of macrophage colony-stimulating factor and its receptor in hepatic granulomas of Kupffer-cell-depleted mice. Am. J. Pathol. *150*, 2047–2060.

Nakamura, K., Ito, T., Yoneda, M., Takamoto, S., Nakade, Y., Okamoto, S., Okada, M., Yokohama, S., Aso, K., and Makino, I. (2002). Antithrombin III prevents concanavalin A-induced liver injury through inhibition of macrophage inflammatory protein-2 release and production of prostacyclin in mice. J. Hepatol. *36*, 766–773.

Noto, K., Kato, K., Okumura, K., and Yagita, H. (1995). Identification and functional characterization of mouse CD29 with a mAb. Int. Immunol. *7*, 835–842.

Ohshima, S., Yamaguchi, N., Nishioka, K., Mima, T., Ishii, T., Umeshita-Sasai, M., Kobayashi, H., Shimizu, M., Katada, Y., Wakitani, S., et al. (2002). Enhanced local production of osteopontin in rheumatoid joints. J. Rheumatol. *29*, 2061–2067.

O'Regan, A.W., Nau, G.J., Chupp, G.L., and Berman, J.S. (2000). Osteopontin (Eta-1) in cell-mediated immunity: teaching an old dog new tricks. Immunol. Today *21*, 475–478.

Ramsaransing, G., Teelken, A., Prokopenko, V.M., Arutjunyan, A.V., and De Keyser, J. (2003). Low leucocyte myeloperoxidase activity in patients with multiple sclerosis. J. Neurol. Neurosurg. Psychiatry *74*, 953–955.

Rittling, S.R., Matsumoto, H.N., McKee, M.D., Nanci, A., An, X.R., Novick, K.E., Kowalski, A.J., Noda, M., and Denhardt, D.T. (1998). Mice lacking osteopontin show normal development and bone structure but display altered osteoclast formation in vitro. J. Bone Miner. Res. *13*, 1101–1111.

Singh, N., Hong, S., Scherer, D.C., Serizawa, I., Burdin, N., Kronenberg, M., Koezuka, Y., and Van Kaer, L. (1999). Cutting edge: activation of NK T cells by CD1d and alpha-galactosylceramide directs conventional T cells to the acquisition of a Th2 phenotype. J. Immunol. *163*, 2373–2377.

Smith, L.L., Cheung, H.K., Ling, L.E., Chen, J., Sheppard, D., Pytela, R., and Giachelli, C.M. (1996). Osteopontin N-terminal domain contains a cryptic adhesive sequence recognized by alpha9beta1 integrin. J. Biol. Chem. *271*, 28485–28491.

Smyth, M.J., Crowe, N.Y., Pellicci, D.G., Kyparissoudis, K., Kelly, J.M., Takeda, K., Yagita, H., and Godfrey, D.I. (2002). Sequential production of interferon-gamma by NK1.1(+) T cells and natural killer cells is essential for the antimetastatic effect of alpha-galactosylceramide. Blood *99*, 1259–1266.

Sodek, J., Ganss, B., and McKee, M.D. (2000). Osteopontin. Crit. Rev. Oral Biol. Med. *11*, 279–303.

Steinman, L., and Zamvil, S. (2003). Transcriptional analysis of targets in multiple sclerosis. Nat. Rev. Immunol. *3*, 483–492.

Takahashi, F., Takahashi, K., Okazaki, T., Maeda, K., Ienaga, H., Maeda, M., Kon, S., Uede, T., and Fukuchi, Y. (2001). Role of osteopontin in the pathogenesis of bleomycin-induced pulmonary fibrosis. Am. J. Respir. Cell Mol. Biol. *24*, 264–271.

Takeda, K., Hayakawa, Y., Van Kaer, L., Matsuda, H., Yagita, H., and Okumura, K. (2000). Critical contribution of liver natural killer T cells to a murine model of hepatitis. Proc. Natl. Acad. Sci. USA *97*, 5498–5503.

Tanaka, K., Morimoto, J., Kon, S., Kimura, C., Inobe, M., Diao, H., Hirschfeld, G., Weiss, J.M., and Uede, T. (2004). Effect of osteopontin alleles on beta-glucan-induced granuloma formation in the mouse liver. Am. J. Pathol. *164*, 567–575.

Taooka, Y., Chen, J., Yednock, T., and Sheppard, D. (1999). The integrin alpha9beta1 mediates adhesion to activated endothelial cells and transendothelial neutrophil migration through interaction with vascular cell adhesion molecule-1. J. Cell Biol. *145*, 413–420.

Tiegs, G., Hentschel, J., and Wendel, A. (1992). A T cell-dependent experimental liver injury in mice inducible by concanavalin A. J. Clin. Invest. *90*, 196–203.

Toyabe, S., Seki, S., Iiai, T., Takeda, K., Shirai, K., Watanabe, H., Hiraide, H., Uchiyama, M., and Abo, T. (1997). Requirement of IL-4 and liver NK1+ T cells for concanavalin A-induced hepatic injury in mice. J. Immunol. *159*, 1537–1542.

Tupin, E., Nicoletti, A., Elhage, R., Rudling, M., Ljunggren, H.G., Hansson, G.K., and Berne, G.P. (2004). CD1d-dependent activation of NKT cells aggravates atherosclerosis. J. Exp. Med. *199*, 417–422.

Yamamoto, N., Sakai, F., Kon, S., Morimoto, J., Kimura, C., Yamazaki, H., Okazaki, I., Seki, N., Fujii, T., and Uede, T. (2003). Essential role of the cryptic epitope SLAYGLR within osteopontin in a murine model of rheumatoid arthritis. J. Clin. Invest. *112*, 181–188.

Yasuda, M., Hasunuma, Y., Adachi, H., Sekine, C., Sakanishi, T., Hashimoto, H., Ra, C., Yagita, H., and Okumura, K. (1995). Expression and function of fibronectin binding integrins on rat mast cells. Int. Immunol. *7*, 251–258.

Yokasaki, Y., and Sheppard, D. (2000). Mapping of the cryptic integrin-binding site in osteopontin suggests a new mechanism by which thrombin can regulate inflammation and tissue repair. Trends Cardiovasc. Med. *10*, 155–159.

Yokosaki, Y., Matsuura, N., Sasaki, T., Murakami, I., Schneider, H., Higashiyama, S., Saitoh, Y., Yamakido, M., Taooka, Y., and Sheppard, D. (1999). The integrin alpha(9)beta(1) binds to a novel recognition sequence (SVVYGLR) in the thrombin-cleaved amino-terminal fragment of osteopontin. J. Biol. Chem. *274*, 36328–36334.

Yoneyama, H., Harada, A., Imai, T., Baba, M., Yoshie, O., Zhang, Y., Higashi, H., Murai, M., Asakura, H., and Matsushima, K. (1998). Pivotal role of TARC, a CC chemokine, in bacteria-induced fulminant hepatic failure in mice. J. Clin. Invest. *102*, 1933–1941.

Yumoto, K., Ishijima, M., Rittling, S.R., Tsuji, K., Tsuchiya, Y., Kon, S., Nifuji, A., Uede, T., Denhardt, D.T., and Noda, M. (2002). Osteopontin deficiency protects joints against destruction in anti-type II collagen antibody-induced arthritis in mice. Proc. Natl. Acad. Sci. USA *99*, 4556–4561.

STAT6-Dependent Differentiation and Production of IL-5 and IL-13 in Murine NK2 Cells[1]

Takuo Katsumoto,* Motoko Kimura,* Masakatsu Yamashita,* Hiroyuki Hosokawa,* Kahoko Hashimoto,† Akihiro Hasegawa,* Miyuki Omori,* Takeshi Miyamoto,* Masaru Taniguchi,‡ and Toshinori Nakayama[2]*

NK cells differentiate into either NK1 or NK2 cells that produce IFN-γ or IL-5 and IL-13, respectively. Little is known, however, about the molecular mechanisms that control NK1 and NK2 cell differentiation. To address these questions, we established an in vitro mouse NK1/NK2 cell differentiation culture system. For NK1/NK2 cell differentiation, initial stimulation with PMA and ionomycin was required. The in vitro differentiated NK2 cells produced IL-5 and IL-13, but the levels were 20 times lower than those of Th2 or T cytotoxic (Tc)2 cells. No detectable IL-4 was produced. Freshly prepared NK cells express IL-2Rβ, IL-2RγC, and IL-4Rα. After stimulation with PMA and ionomycin, NK cells expressed IL-2Rα. NK1 cells displayed higher cytotoxic activity against Yac-1 target cells. The levels of GATA3 protein in developing NK2 cells were approximately one-sixth of those in Th2 cells. Both NK1 and NK2 cells expressed large amounts of repressor of GATA, the levels of which were equivalent to CD8 Tc1 and Tc2 cells and significantly higher than those in Th2 cells. The levels of histone hyperacetylation of the IL-4 and IL-13 gene loci in NK2 cells were very low and equivalent to those in naive CD4 T cells. The production of IL-5 and IL-13 in NK2 cells was found to be STAT6 dependent. Thus, similar to Th2 cells, NK2 cell development is dependent on STAT6, and the low level expression of GATA3 and the high level expression of repressor of GATA may influence the unique type 2 cytokine production profiles of NK2 cells. *The Journal of Immunology*, **2004, 173: 4967–4975.**

Natural killer cells produce IFN-γ upon IL-2 stimulation and play crucial roles during infection and in anti-tumor immunity (1, 2). However, human NK cells are known to produce type 2 cytokines as well, particularly when cultured with certain cytokines (3–7). NK1/NK2 terminology has been proposed in analogy to Th1/Th2 subsets of CD4 T cells (4). The roles of NK2 cells in host defense immune responses remain undetermined; however, the unique cytokine production profile of NK2 cells suggests that these cells may play certain roles in specific immune responses, including the regulation of allergic or autoimmune diseases (8–10).

The molecular requirements for the differentiation of functional type 1 and type 2 cytokine-producing Th1/Th2 cells have been extensively investigated. The IL-12-mediated activation of STAT4 is required for Th1 cell differentiation, and IL-4-mediated STAT6 activation is crucial for Th2 cell differentiation (11–14). In addition to cytokine-mediated signals, activation of TCR-mediated signaling is also indispensable for both Th1 and Th2 cell differentiation (15–17). Master transcription factors for Th1 and Th2 cell differentiation have been revealed, i.e., GATA3 for Th2 and T-bet for Th1 (18–21).

Changes in the chromatin structure of the Th2 cytokine (IL-4/IL-5/IL-13) gene loci occur during Th2 cell differentiation (22). Hyperacetylation of histones H3 and H4 by histone acetyl transferases has been suggested to be associated with active chromatin (23). Recently, we and others have reported that hyperacetylation of histone H3 and H4 tails of nucleosomes associated with the Th2 cytokine gene loci occurs in developing Th2 cells, but not in naive or developing Th1 cells (24–26).

In the present study we established an in vitro murine NK1/NK2 cell differentiation system and demonstrate molecular events that may govern the unique cytokine production of NK1/NK2 cells. NK1 cells produced substantial amounts of IFN-γ with hyperacetylation of the IFN-γ promoter locus. Interestingly, NK2 cells produced low levels of IL-5 and IL-13 and undetectable levels of IL-4. This unique profile appears to be due to the low level expression of GATA3 and the high level expression of repressor of GATA (ROG)[3] in developing NK2 cells. Type 2 cytokine production in NK2 cells was found to be STAT6 dependent.

Materials and Methods

Mice

C57BL/6 mice were purchased from Charles River Laboratories (Tokyo, Japan). STAT6-deficient mice (27) were provided by Dr. S. Akira (Osaka University, Japan). RAG1-deficient mice were purchased from Jackson Laboratory (Bar Harbor, ME). All mice were maintained under specific

*Department of Immunology, Graduate School of Medicine, Chiba University, and †Department of Life and Environmental Sciences and High Technology Research Center, Chiba Institute of Technology, Chiba, Japan; and ‡Laboratory for Immune Regulation, RIKEN Research Center for Allergy and Immunology, Yokohama, Japan

Received for publication December 18, 2003. Accepted for publication August 5, 2004.

The costs of publication of this article were defrayed in part by the payment of page charges. This article must therefore be hereby marked *advertisement* in accordance with 18 U.S.C. Section 1734 solely to indicate this fact.

[1] This work was supported by grants from the Ministry of Education, Culture, Sports, Science, and Technology of Japan (Grants-in-Aid for Scientific Research, Priority Areas Research 13218016 and 12051203; Scientific Research B 14370107, Advanced and Innovational Research Program in Life Science; and Special Coordination Funds); the Ministry of Health, Labor, and Welfare of Japan (a grant-in-aid for research on Advanced Medical Technology); the Program for Promotion of Fundamental Studies in Health Science of the Organization for Pharmaceutical Safety and Research of Japan; The Hamaguchi Foundation; and The Uehara Memorial Foundation.

[2] Address correspondence and reprint requests to Dr. Toshinori Nakayama, Department of Immunology, Graduate School of Medicine, Chiba University, 1-8-1 Inohana, Chuo-ku, Chiba 260-8670, Japan. E-mail address: tnakayama@faculty.chiba-u.jp

[3] Abbreviations used in this paper: ROG, repressor of GATA; Cγ, common γ-chain; ChIP, chromatin immunoprecipitation; EGFP, enhanced GFP; IRES, internal ribosome entry site; Tc, T cytotoxic.

0022-1767/04/$02.00

pathogen-free conditions and used for experiments when ~7 wk old. Animal care was in accordance with the guidelines of Chiba University.

Reagents

The reagents used in this study were as follows: Cy5-conjugated streptavidin was prepared in our laboratory. Anti-NK1.1-FITC (PK136-FITC), anti-CD4-FITC (RM4-5-FITC), anti-CD11b-FITC (M1/70-FITC), anti-CD44-FITC (IM7-FITC), anti-CD69-FITC (H1.2F3-FITC), anti-CD95-FITC (Jo2-FITC), anti-Ly49A-FITC (A-1-FITC), anti-Ly49D-FITC (4E5-FITC), anti-TCR$\alpha\beta$-PE (H57-597-PE), anti-CD4-PE (RM4-5-PE), anti-CD8α-PE (53-6.7-PE), anti-CD25-PE (7D4-PE), anti-CD122-PE (TM-β1-PE), anti-CD124-PE (mIL4R-M1-PE), anti-CD132-PE (4G3-PE), anti-CD11b-biotin (M1/70-biotin), anti-CD94-biotin (18d3-biotin), anti-CD119-biotin (GR20-biotin), anti-CD178-biotin (MFL4-biotin), anti-CD212-biotin (114-biotin), anti-NK1.1-allophycocyanin (PK136-allophycocyanin), anti-CD25-PE (7D4-PE), anti-CD122-PE (TM-β1-PE), anti-CD124-PE (mIL4R-M1-PE), and anti-CD132-PE (4G3-PE) were purchased from BD Pharmingen (La Jolla, CA). Streptavidin-FITC was purchased from Biomeda (Foster City, CA). Anti-FcRγII/II mAb (2.4G2), anti-IFN-γ mAb (RA2.6A2), and anti-IL-4 mAb (11B11) were used as culture supernatants.

Immunofluorescent staining and flow cytometric analysis

In general, one million cells were preincubated with 2.4G2 to prevent nonspecific binding of mAb via FcR interactions, then incubated on ice for 30 min with the appropriate staining reagents according to a standard method previously described (28). Flow cytometric analysis was performed on a FACSCalibur (BD Biosciences, Mountain View, CA), and the results were analyzed with CellQuest software (BD Biosciences).

^{51}Cr release cytotoxic assay

The cytotoxic activities of differentiated NK cells were assessed by a 4-h ^{51}Cr release cytotoxic assay using the Yac-1 lymphoma cell line as previously described (29). The cells were harvested and seeded at the indicated E:T cell ratios. Specific lysis was calculated according to the following formula: % specific lysis = 100 × ([experimental cpm − spontaneous cpm]/[maximum cpm − spontaneous cpm]).

ELISA for the measurement of cytokine concentration

Differentiated NK cells (0.2×10^6) were stimulated with IL-2 (500 U/ml) or PMA (50 ng/ml) and ionomycin (500 nM) for 72 h in 200-μl cultures. The production of IL-4, IL-5, and IFN-γ was measured by ELISA as previously described (30). The productions of IL-10 and IL-13 were measured using a mouse IL-10 BD OptEIA ELISA Kit (BD Biosciences) and mouse IL-13 ELISA kit (R&D Systems, Minneapolis, MN) respectively, according to the manufacturers' protocols.

In vitro NK and T cell differentiation culture

NK cells (NK1.1$^+$/TCR$\alpha\beta^-$ cells) were isolated from spleens using magnetic beads and an AutoMACS sorter (Miltenyi Biotec, Auburn, CA), then sorted on a FACSVantage cell sorter (BD Biosciences), yielding a purity of >98%. Purified NK cells (2.0×10^6) were stimulated for 2 days with PMA (50 ng/ml) and ionomycin (500 nM) in the presence of IL-2 (250 U/ml) for neutral (NK0-skewed) conditions, IL-2 (250 U/ml) and IL-12 (500 U/ml) for NK1-skewed conditions, and IL-2 (250 U/ml), IL-4 (500 U/ml), and anti-IFN-γ mAb (R4.6A2, 25% culture supernatant) for NK2-skewed conditions. The cells were then transferred to new dishes and cultured for another 5–7 days in the presence of only the cytokines present in the initial culture. IL-18 was purchased from eBioscience. IFNα and IFNβ were purchased from PeproTech (Rocky Hill, NJ).

Culture conditions for Th1/Th2 and T cytotoxic (Tc)1/Tc2 differentiation were described previously (24, 30). In brief, CD4 T and CD8 T cells were purified using magnetic beads and an AutoMACS sorter (Miltenyi Biotec), yielding a purity of >98%. Enriched CD4 T and CD8 T cells (2.0×10^6) were stimulated for 2 days with 1 μg/ml immobilized anti-TCR mAb (H57-597) in the presence of IL-2 (25 U/ml), IL-12 (100 U/ml), and anti-IL-4 mAb (11B11, 25% culture supernatant) for type 1-skewed conditions and in the presence of IL-2 (25 U/ml) and IL-4 (100 U/ml) for type 2-skewed conditions. The cells were then transferred to new dishes and cultured for another 3 days in the presence of only the cytokines present in the initial culture.

Chromatin immunoprecipitation (ChIP) assay

ChIP was performed using a histone H3 ChIP assay kit (no. 17-245: Upstate Biotechnology, Lake Placid, NY). The primers used for PCR amplification were described previously (24). Images were quantified using an L&S analyzer (ATTO, Tokyo, Japan).

PCR

Total RNA was isolated using TRIzol reagent (Invitrogen Life Technologies, Gaithersburg, MD). RT was performed using Superscript II (Invitrogen Life Technologies-BRL). Three-fold serial dilutions of template cDNA

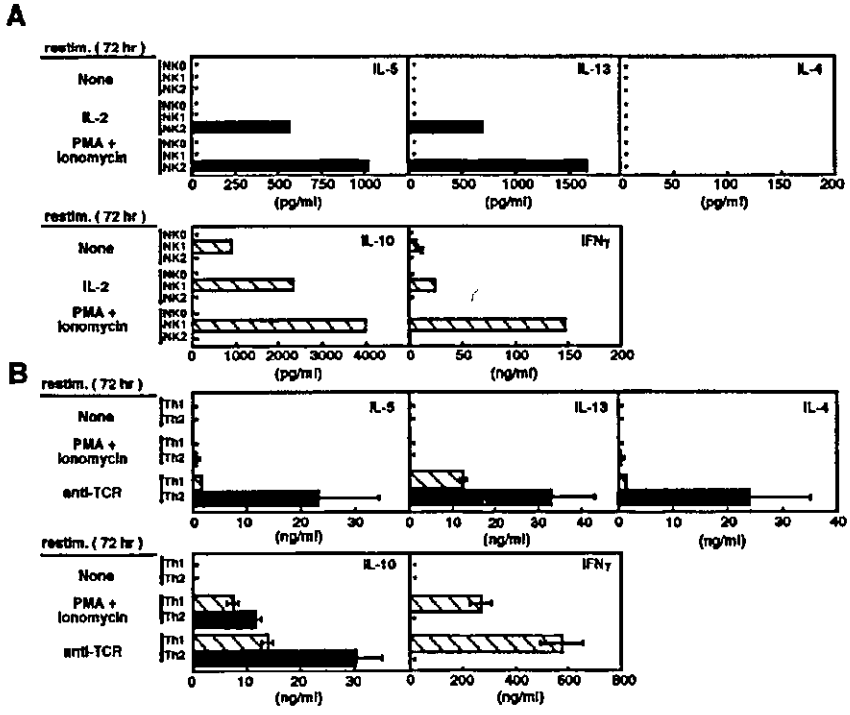

FIGURE 1. Cytokine production profiles of NK0, NK1, and NK2 cells differentiated in vitro. *A*, NK1.1$^+$/TCR$\alpha\beta^-$ NK cells purified from the spleen (>98%) were differentiated under NK0-, NK1-, and NK2-skewed conditions for 8 days. The cultured NK cells were washed extensively and restimulated with IL-2 (500 U/ml) or PMA (50 ng/ml) plus ionomycin (500 nM) for 72 h, and the production of IL-5, IL-13, IL-4, IL-10, and IFN-γ in the culture supernatant was assessed by ELISA. □, NK0 cells; ▨, NK1 cells, ■, NK2 cells. Three independent experiments were performed with similar results. *B*, Freshly prepared splenic CD4 T cells from C57BL/6 mice were cultured under type 1- and type 2-skewed conditions for 5 days. Cultured T cells were restimulated with immobilized anti-TCR mAb for 72 h, and the amounts of IL-5, IL-13, IL-4, IFN-γ, and IL-10 in the culture supernatant were assessed by ELISA. ▨, Th1 cells; ■, Th2 cells. *, Not detectable.

were achieved as previously described (31). The primers used in the RT-PCR study were as follows: β-actin forward, GAGAG GGAAATCGTGCGTGA-3′; β-actin reverse, 5′-ACATCTGCTGGAAGGTGGAC; GATA3 forward, GAAGGCATCCAGACCCGAAAC-3′; GATA3 reverse, 5′-ACCCATGG CGGTGACCATGC; ROG forward, CTCTCTGGAGTCAGAATC AGCTGG-3′; ROG reverse, 5′-AGCGCTGAGGACAGAGGCTACAGG; IL-12Rβ2 forward, ACATCCAATAAGCAGCCTACAGCC-3′; IL-12Rβ2 reverse, 5′-GGCCATGCCATCAGGAGATTATCC; granzyme B forward, GCCCACAACTGCTGGAAGAACAG-3′; granzyme B reverse, 5′-AAC CAGC CACATAGCACACAT; perforin 1 forward, TGCTACACTGCCA CTCGGTCA-3′; perforin 1 reverse, 5′-TTGGCTACCTTGGAGTGGGAG; GATA1 forward, CATTGGCCCCTTGTGAGGCCAGAGA-3′; GATA1 reverse, 5′-ACCTGATGG AGCTTGAAATAGAGGC; GATA2 forward, GCCTGTGGCCTCTACTACAA GCTG-3′; and GATA2 reverse, 5′-CCATGGCAGTCACCATGCTGGACG.

For real-time PCR, a TaqMan universal PCR master mix was used for all reactions (Applied Biosystems) and the ABI PRISM 7000 Sequence Detection System was used. The primers and TaqMan probes for the detection of T-bet and hypoxanthine phosphoribosyltransferase were purchased from Applied Biosystems. T-bet expression was normalized using the hypoxanthine phosphoribosyltransferase signal. Data are shown as relative intensity.

Retrovirus vectors and infection

The pMx-internal ribosome entry site (IRES)-GFP and the Plat-E packaging cell line were provided by Dr. T. Kitamura (University of Tokyo, Tokyo, Japan); pMx-IRES-GFP and pMx-GATA3-IRES-GFP and the methods for the generation of virus supernatants were described previously (30). The LFD-14 cell line (32) was provided by Dr. N. Minato (Kyoto University, Kyoto, Japan) and was maintained in the presence of IL-2 (100 U/ml). LFD14 cells were infected with pMx-GATA3-IRES-GFP, cultured for 2 days, and harvested, and the GFP-positive cells were isolated by sorting on a FACSVantage cell sorter (BD Biosciences). GFP-positive cells were cultured for another 2 days, then restimulated with IL-2 (500 U/ml) or PMA (50 ng/ml) plus ionomycin (500 nM) for 72 h in 200-μl cultures.

Immunoblot analysis

Nuclear extracts for the detection of GATA3 and ROG, and cytoplasmic extracts for tubulin-α were prepared using NE-PER Nuclear and Cytoplasmic Extraction Reagent (catalogue no. 78833; Pierce, Rockford, IL). Immunoblotting was performed with anti-GATA3 mouse mAb (HG3-31; Santa Cruz Biotechnology, Santa Cruz, CA), anti-tubulin-α mouse mAb (DM1A; Neo Markers, Fremont, CA) and anti-ROG rabbit antisera as described previously (30). Protein levels were visualized by ECL (Amersham Biosciences, Arlington Heights, IL) using HRP-conjugated anti-mouse Ig Ab (Amersham Biosciences).

Results

Cytokine production profiles of NK0, NK1, and NK2 cells differentiated in vitro

The aim of this study was to clarify the molecular events underlying NK1/NK2 cell differentiation. We first established an in vitro murine NK1/NK2 cell differentiation system without feeder cells. Purified splenic NK cells were stimulated with PMA plus ionomycin for 2 days under NK0-, NK1-, and NK2-skewed culture conditions, then the cells were transferred to new wells to culture for another 6 days with the cytokines present in the initial culture. The amounts of cytokines produced by in vitro differentiated NK0, NK1, and NK2 cells after IL-2 or PMA plus ionomycin restimulation were assessed by ELISA (Fig. 1*A*). We designated NK0 cells as NK cells cultured under non-type 1- or non-type 2-skewed conditions as described in *Materials and Methods*. As expected, the production of IL-5 and IL-13 was detected only in NK2 cells. No IL-4 production was detected. The amounts of IL-5 and IL-13 produced by NK2 cells were ~20-fold less than those produced by Th2 cells (Fig. 1). Only NK1 cells produced IL-10 and IFN-γ. The levels of IFN-γ produced by NK1 cells were significantly lower than those produced by Th1 cells (Fig. 1). We performed cytoplasmic cytokine staining, but could not detect significant IL-5- or IL-13-producing populations in the NK2 cell population (data not shown). This is probably due to the low sensitivity of the system, but the result suggests that the limited amounts of IL-5 and IL-13 detected by ELISA are not produced by a small population secreting very high amounts of IL-13 and IL-5. Taken together, these results suggest that in vitro differentiated mouse NK1 and NK2 cells possess unique cytokine production profiles.

Effects of IL-18, IL-12, IFN-α, and IFN-β on the production of IFN-γ in NK cells

NK1 cells prepared as described in Fig. 1 were stimulated with PMA plus ionomycin, IL-18, IFN-α, IFN-β, or IL-12, and the amounts of IFN-γ produced in the culture supernatant were measured by ELISA. As shown in Fig. 2*A*, IL-18 induced substantial amounts of IFN-γ in NK1 cells. IL-12 induced levels of IFN-γ production similar to those induced by PMA and ionomycin. The effects of IFN-α or IFN-β were less than those of IL-12. In addition, the effects of IL-18 in NK cell differentiation culture were assessed. NK cells were cultured in the presence of IL-2 (NK0 conditions), IL-2 plus IL-12 (NK1 conditions), or IL-2 plus IL-18 (50 ng/ml), then the cells were restimulated with IL-2 or PMA plus ionomycin. The addition of IL-12 enhanced the production of IFN-γ, but no significant effect of IL-18 was observed (Fig. 2*B*).

Cell surface expression of cytokine receptors and NK cell-related marker Ags in fresh, activated, and differentiated NK cell subsets

To characterize the purified NK cells, we first assessed their cell surface expressions of IL-2Rα, IL-2Rβ, common γ-chain (γC), and IL-4Rα (Fig. 3*A*). Considerable levels of IL-2Rβ, γC, and

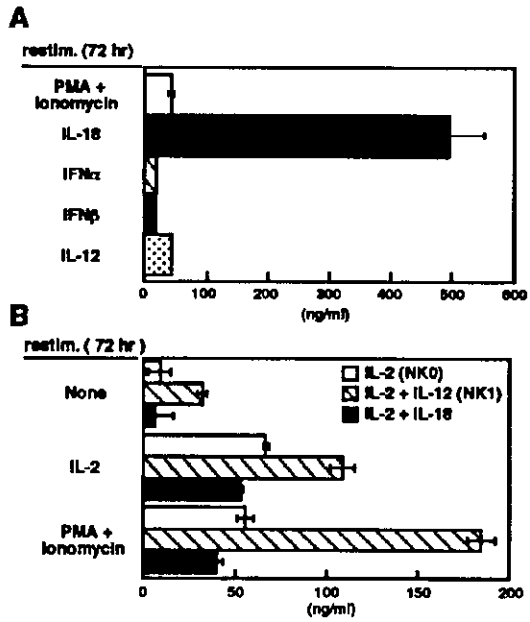

FIGURE 2. IFN-γ production by NK1 cells stimulated with various cytokines. *A*, NK1 cells were prepared as described in Fig. 1 and restimulated with PMA plus ionomycin, IL-18 (50 ng/ml), IFN-α (1000 U/ml) and IFN-β (1000 U/ml), or IL-12 (500 U/ml) for 72 h, then the amounts of IFN-γ produced in the culture supernatant were assessed by ELISA. *B*, Purified NK cells were cultured in the presence of IL-2 (NK0 conditions), IL-2 plus IL-12 (NK1 conditions), or IL-2 plus IL-18 (50 ng/ml). The cultured NK cells were washed extensively and restimulated as described in Fig. 1*A*, and the production of IFN-γ in the culture supernatant was assessed by ELISA.

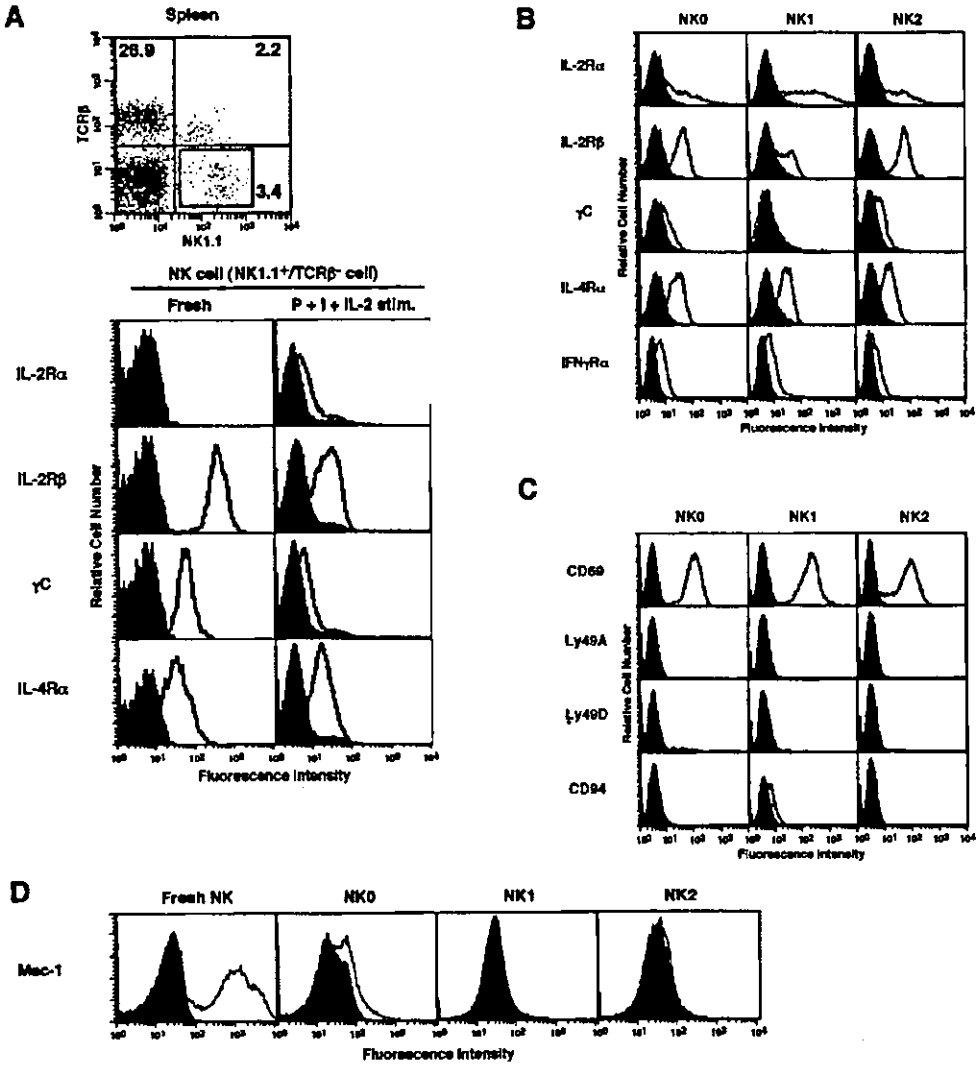

FIGURE 3. Cell surface expression profiles of cytokine receptors and NK cell-related marker Ags in fresh and differentiated NK cell subsets. *A*, Representative NK1.1/TCRβ staining profiles in splenocytes (*upper panel*) and the indicated cytokine receptor components on electronically gated NK1.1$^+$/TCRβ^- NK cells from freshly isolated splenocytes and from splenocytes stimulated for 1 day with PMA (50 ng/ml) and ionomycin (500 nM) in the presence of IL-2 (250 U/ml; *lower panel*). Background staining is shown as filled areas. *B–D*, Cell surface expression of the indicated molecules on freshly prepared NK, NK0, NK1, and NK2 cells. NK1.1$^+$/TCR$\alpha\beta^-$ NK cells purified from the spleen (>98%) were differentiated under NK0-, NK1-, or NK2-skewed conditions for 8 days. The cultured NK cells were washed extensively and subjected to flow cytometric analysis. Background staining is shown as shaded areas.

IL-4Rα were expressed on freshly prepared NK cells, whereas IL-2Rα was undetectable. In NK cells activated by stimulation with PMA plus ionomycin and IL-2 for 1 day, IL-2Rα, IL-2Rβ, γC, and IL-4Rα were all expressed (Fig. 3*A*). Next, the staining profiles of cytokine receptors in NK0, NK1, and NK2 cells were determined. As shown in Fig. 3*B*, all cytokine receptor components were expressed on NK0 and NK2 cells, whereas a significantly lower expression of IL-2Rβ and undetectable expression of γC were found in NK1 cells. Fig. 3*C* shows the staining profiles of various surface marker Ags. An activation marker, CD69, was expressed on every subset of NK cells. No significant Ly49A and Ly49D staining was observed in either subset of NK cells. CD94 was slightly expressed only on NK1 cells. The level of Mac-1 (CD11b) expression, which reportedly correlates with NK cell maturation, was high on freshly prepared NK cells (Fig. 3*D*). The expression was down-regulated during NK cell differentiation. No significant staining of Mac-1 was detected on NK1 cells.

Cytotoxic function of differentiated NK cell subsets

The cytotoxic activity of differentiated NK cells was measured by a standard 4-h Cr release assay with Yac-1 target cells. As shown in Fig. 4, all NK cell subsets displayed significant levels of cytotoxic activity to Yac-1 cells. Among them, NK0 cells expressed the highest levels of cytotoxic activity, and NK2 cells showed the lowest cytotoxic activity. NK1 cells produced higher amounts of IFN-γ, but the levels of cytotoxic activity were similar to those of fresh NK cells. In freshly prepared NK cells, only low level IFN-γ

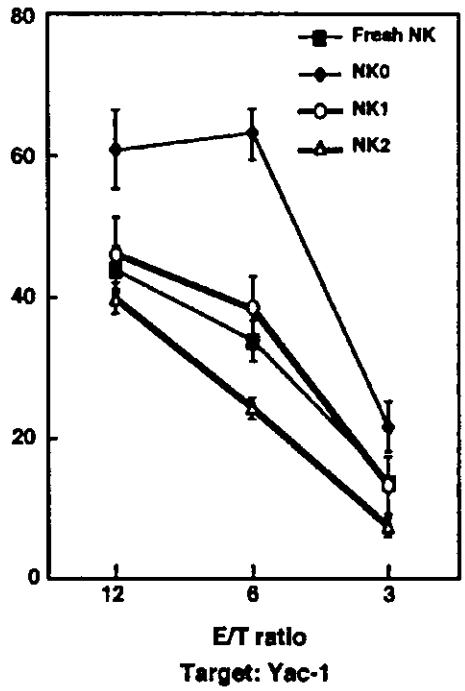

FIGURE 4. Cytotoxic activity of differentiated NK cells. Freshly prepared purified NK cells and NK0, NK1, and NK2 cells differentiated in the 7-day cultures were subjected to the standard ^{51}Cr release cytotoxic assay in triplicate with target Yac-1 lymphoma cells. The mean percent cytotoxicity and SD are shown. Three independent experiments were performed with similar results.

production (~10 ng/ml; <1/10th of NK1) was detected upon stimulation with PMA plus ionomycin (data not shown). These results suggest no clear link between the production of IFN-γ and cytotoxic activity.

Expression of GATA3, GATA2, GATA1, ROG, granzyme B, perforin 1, and IL-12Rβ2 in differentiated NK subsets

Next, to examine the genes that may regulate NK1/NK2 cell differentiation and cytokine production, we studied the mRNA expression of various transcription factors and a cytokine receptor in NK cells compared with that in Th1/Th2 (Fig. 5*A*) and Tc1/Tc2 cells (Fig. 5*B*). Bone marrow-derived mast cells were used as a control for GATA1 and GATA2. GATA3, a crucial factor for Th2 cell differentiation, was expressed at a significantly higher level in NK2 cells than in freshly prepared NK, NK0, or NK1 cells. The levels were equivalent to those in naive CD4, Th1, or Tc2 cells and were significantly lower than those in Th2 cells. Neither GATA1 nor GATA2 was expressed in these NK cells. ROG plays crucial roles in cytokine expression and chromatin remodeling in developing Tc2 cells (30). Interestingly, ROG was found to be highly expressed in NK0, NK1, and NK2 cells, with expression levels equivalent to those in Tc1 and Tc2 cells. Thus, the low level production of type 2 cytokines (IL-5 and IL-13) in NK2 cells appears to be due in part to the low level of GATA3 induction. In addition, the lack of detectable IL-4 production in NK2 cells may be due to both the low level induction of GATA3 and the high level expression of ROG. This is reminiscent of the unique type 2 cytokine production profiles of CD8 T cells (30).

Simultaneously, we studied the expression levels of IL-12Rβ2, perforin 1, and granzyme B in differentiated NK cells. Substantial levels of the mRNAs for granzyme B, perforin 1, and IL-12Rβ2 were detected in NK0, NK1, and NK2 cells, but not in freshly prepared NK cells. The expression levels of IL-12Rβ2 in NK1 cells were about half those in NK0 or NK2 cells (Fig. 5*A*).

The protein expression levels of GATA3 and ROG were assessed by immunoblotting analysis in fresh NK, in vitro differentiated NK2, and Th2 cells using specific Abs (Fig. 5*C*). NK2 cells expressed significant amounts of GATA3, although the levels were much less than those in Th2 cells. Considerable levels of ROG protein were detected in NK2 cells, but not in fresh NK or Th2 cells.

Next, we performed real-time PCR analysis on T-bet expression in freshly prepared NK cells, NK0, NK1, and NK2 cells; naive CD4 T cells; Th1 and Th2 cells; naive CD8 T cells; and Tc1 and Tc2 cells (Fig. 5*D*). The level of T-bet transcription was highest in fresh NK cells. NK0, NK1, and NK2 cells expressed significant, but similar, levels of T-bet. The levels were higher than those of naive CD4 and CD8 cells or Th2 and Tc2 cells, but lower than those of Th1 or Tc1 cells. These results suggest that there is no correlation between the production of IFN-γ or type 2 cytokines and the expression levels of T-bet transcription in NK0, NK1, and NK2 cells.

Acetylation status of the IFN-γ and type 2 cytokine gene loci in differentiated NK cell subsets

Next, we investigated the acetylation status of histones associated with the IFN-γ and type 2 cytokine gene loci. A ChIP assay using anti-histone H3 mAb was performed with titrated doses of DNA samples. Fig. 6*A* shows the real-time quantitative PCR bands derived from freshly prepared NK, NK1, and NK2 cells; freshly prepared naive CD4 and Th2 cells; and those of input DNA. The results of this analysis are presented as the relative intensity of each group normalized to the band intensity of the corresponding input DNA bands (Fig. 6*B*). The acetylation levels of the type 2 cytokine gene loci (IL-4 promoter, IL-13 promoter, IL-4 V_A enhancer, conserved noncoding sequence 1, and conserved GATA response element) in NK2 cells were clearly lower than those in Th2 cells, and almost the same as those in naive CD4 T cells. As for the IL-5 locus, acetylation of histones was not fully induced (~2-fold) in Th2 cells on day 5, and the acetylation levels in NK cell subsets were equivalent to those in Th2 cells. The acetylation levels of the IFN-γ promoter locus were higher in NK1 cells compared with those in NK2 cells or Th2 cells. The levels were approximately one-third those in Th1 cells (data not shown). Thus, the cytokine production profiles of NK1 and NK2 cells appear to reflect the acetylation status of histones associated with the IFN-γ and type 2 cytokine gene loci.

STAT6 is required for NK2 cell differentiation

To investigate the requirement of STAT6 for NK2 cell differentiation, we prepared NK cells from STAT6-deficient mice. The number of NK cells in the spleen and the expressions of NK cell surface markers, such as those shown in Fig. 3, were all equivalent to those of wild-type C57BL/6 NK cells (data not shown). As shown in Fig. 7*A*, the STAT6-deficient NK cells cultured under type 2-skewed conditions did not produce detectable levels of IL-5 or IL-13. The production of IFN-γ was not decreased, but was slightly increased, in STAT6-deficient NK1 cells. These results suggest that NK2 cell differentiation is STAT6 dependent.

Ectopic expression of GATA3 in an NK-like cell line induces IL-13 production upon IL-2 stimulation

Finally, we studied whether the ectopic expression of GATA3 induces the production of type 2 cytokines in NK cells. Because the

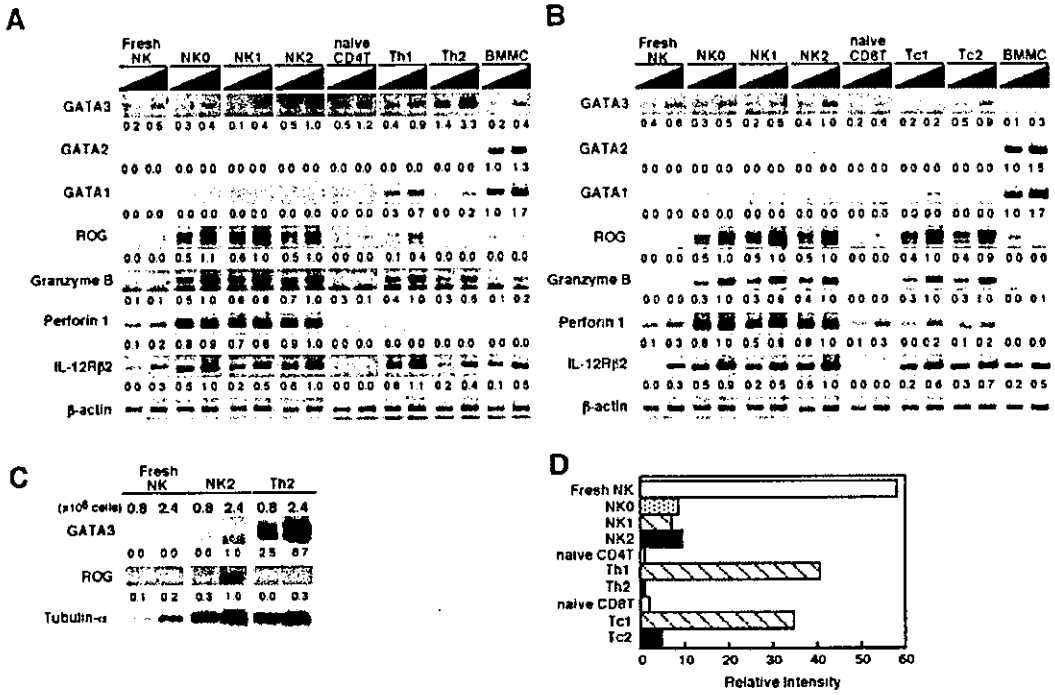

FIGURE 5. Expression of GATA3, GATA2, GATA1, ROG, granzyme B, perforin 1, and IL-12Rβ2 in differentiated NK cell subsets. Purified NK cells were cultured under each condition for 7 days. CD4 and CD8 T cells were cultured under type 1- or type 2-skewed conditions for 5 days. Total RNA was extracted from the cultured cells, and the mRNA levels of the indicated genes were determined by semiquantitative RT-PCR analysis with 3-fold serial dilution of template DNA. Samples from cultured NK cells and CD4 T cells (*A*) or from cultured NK cells and CD8 T cells (*B*) were run on the same gel. Shown are the PCR product bands for each primer pair. The intensities of the bands were measured by densitometry. Quantitative representations of the results indicated under each band were normalized to β-actin, and the relative intensities in each primer pair are shown under each band. For GATA1 and GATA2, relative intensities (each band/the lower concentration band of bone marrow-derived mast cells (BMMC)) are shown. Three independent experiments were performed with similar results. *C*, The amounts of GATA3, ROG, and tubulin-α protein in freshly prepared NK cells, differentiated NK2 cells, and Th2 cells were determined by immunoblotting with specific Abs. Lysates of 2.4×10^6 (*right lane*) and 0.8×10^6 (*left lane*) cells were loaded per lane. Quantitative representations of the results indicated under each band were normalized to tubulin-α, and the relative intensities are shown. *D*, The levels of T-bet transcription in the indicated cell populations were determined by real-time PCR analysis. Total RNA was extracted from the cultured cells as described in *A*, and the mRNA levels of T-bet were determined by real-time RT-PCR analysis. Two independent experiments were performed with similar results.

naive or activated splenic NK cells were resistant to retrovirus infection, we used the fetal liver-derived NK-like cell line LFD14. LFD14 cells were infected with a retrovirus encoding GATA3 bicistronically with enhanced GFP (EGFP). Two days after infection, enhanced GFP-positive cells were isolated, cultured for another 2 days, harvested, and restimulated with IL-2 or PMA plus ionomycin for 72 h. The production of type 2 cytokines (IL-4, IL-5, and IL-13) was measured by ELISA. As shown in Fig. 7*B*, IL-13 was detected in GATA3-transfected LFD14 cells after IL-2 stimulation, whereas no IL-4 and IL-5 were detected. Fig. 7*C* shows the increased expression of GATA3 in the GATA3-infected LFD14 cells, suggesting that the ectopic expression of GATA3 induces IL-13 production in NK-like LFD14 cells. As in the case of differentiated NK0, NK1, and NK2 cells, LFD14 cells expressed significant amounts of ROG protein.

Discussion

In this study we established an in vitro murine NK1/NK2 cell differentiation system and demonstrated molecular requirements that may govern the unique cytokine production of NK1/NK2 cells. In particular, NK2 cells produce low levels of IL-13 and IL-5 and undetectable levels of IL-4. These unique profiles may be associated with the low level expression of GATA3 and the high level expression of ROG in developing NK2 cells. The levels of acetylation at the type 2 cytokine gene loci in NK2 cells were clearly lower than those in Th2 cells, a finding consistent with the levels of type 2 cytokine production. The production of IL-13 and IL-5 by NK cells was revealed to be STAT6 dependent.

We established a mouse NK1/NK2 cell differentiation culture system in which NK cells were stimulated with PMA and ionomycin in the presence of IL-2. IL-12 and IL-4 were used for type 1- and type 2-skewed differentiation. No feeder cells were used in the culture. Stimulation with PMA and ionomycin at the initial phase of culture was indispensable for the induction of NK1/NK2 cells. Previous studies have shown that human NK cells differentiate into NK1 or NK2 cells after cultivation with gamma-irradiated feeder cells or NK-sensitive tumor cells in the presence of IL-2 or IL-15 (4–6). In these human systems, it is possible that the feeder cells or NK-sensitive tumor cells may substitute the activation of both Ca^{2+}/calcineurin and the Ras-MAPK signaling pathway. In fact, it is known that the cross-linking of CD16 on NK cells induces the activation of calcineurin and subsequent NFAT activation (33) and activation of the ERK/MAPK cascade (34). In any event, the requirement for the activation of both Ca^{2+}/calcineurin and the Ras-MAPK signaling pathway for NK1 and NK2 cell differentiation is reminiscent of the differentiation of Th cells. Ag-induced, TCR-mediated signaling in naive T cells is indispensable for the differentiation of Th1/Th2 cells. We have reported that

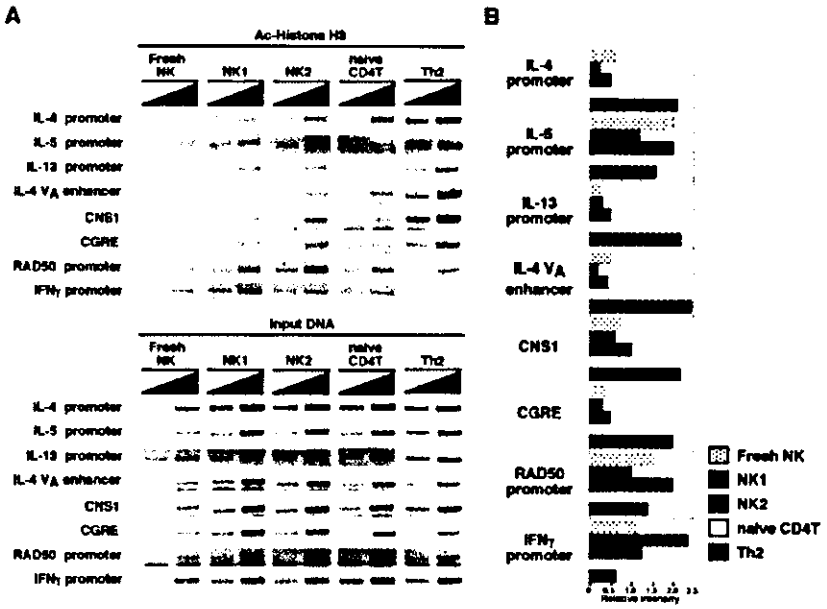

FIGURE 6. Acetylation status of the IFN-γ and type 2 cytokine gene loci in differentiated NK1 and NK2 cells. *A*, Purified NK cells and CD4 T cells were cultured under type 1- or type 2-skewed conditions for 5 days, and ChIP assays were performed. PCR was performed with 3-fold serial dilutions of template cDNA. Shown are the PCR product bands for each primer pair. The results of input DNA are shown in parallel. *B*, Quantitative representation of the results shown in *A*. The intensities of the bands were measured by densitometry. The relative intensity (anti-acetylhistone-H3 precipitated/input DNA ratio) in each primer pair is shown. The results are representative of three experiments.

efficient activation of calcineurin (17) and the Ras-MAPK signaling pathway (16) are crucial for Th2 cell differentiation. This interesting analogy may suggest that even in NK2 cells, the strength of the signaling events may influence the direction of differentiation toward NK1 and NK2 cells. Indeed, our preliminary results suggest that decreased doses of PMA plus ionomycin abrogate NK2 cell differentiation, but not NK1 cell differentiation (unpublished observations).

We and others (4) have observed that in vitro differentiated NK2 cells produce significant amounts of IL-13 and IL-5 even after resting in culture for 4–7 days. In addition, although the system is slightly different, $NK1.1^+CD3^-$ NK cells differentiated from lineage-negative bone marrow cells by culture with feeder cells, IL-2, and IL-15 produced IL-5 and IL-13 (5). Thus, we think the IL-5- and IL-13-producing NK cells are not just a transient state induced by the constant present of IL-4 in the culture, but are a truly differentiated cell population with a self-sustainable phenotype.

The low level production of IL-5 and IL-13 and undetectable production of IL-4 in developing NK2 cells may be partly due to the low levels of GATA3 expression in NK cells. The expression levels of GATA3 in NK2 cells were less than those in Th2 cells. Other GATA family members, GATA1 and GATA2, were not expressed in these NK cell subsets (Fig. 5). Th2 cell differentiation is known to be highly dependent on the expression levels of GATA3 (18). In addition, GATA3 is important as a transcription factor for the type 2 cytokine genes, particularly for activation of the IL-13 and IL-5 genes (18, 35, 36). Thus, it is possible that the low level production of IL-5 and IL-13 is due to a defect at the transcriptional phase, but not at the differentiation phase. However, we detected impaired histone hyperacetylation of the type 2 cytokine gene loci (Fig. 6), suggesting that the limited GATA3 expression affects chromatin remodeling at the differentiation phase.

Another interesting finding in developing NK cells is the high level expression of ROG (Fig. 5). ROG was originally reported to be a repressor of GATA3-induced transactivation of the IL-4 and IL-5 promoters in the M12 B and EL-4 T cell lines by preventing GATA3 from binding to DNA (37). GATA3 is required for chromatin remodeling of the IL-4 and IL-13 gene loci (24) and the IL-5 gene locus (38). The levels of transcription of the IL-5 and IL-13 genes are highly dependent on GATA3. Thus, as for the limited production of three Th2 cytokines (IL-5, IL-13, and IL-4) in NK2 cells, their high level expression of ROG may contribute significantly by inhibiting GATA3 function very efficiently. Another possible mechanism responsible for undetectable production of IL-4 in NK2 cells is ROG-mediated inhibition of chromatin remodeling in the IL-4 gene locus. Recently, we reported that the expression of ROG is much higher in CD8 T cells than in CD4 T cells and provided evidence suggesting that the high level expression of ROG causes limited production of IL-4 in Tc2 cells (30). ROG may bind to the conserved ROG response element in IL-13 exon 4 and recruit histone deacetylase 1 and 2 at this element, resulting in the inhibition of histone hyperacetylation in the region downstream of the IL-13 gene, including the IL-4 locus (30). In NK2 cells, ROG was expressed at a high level, similar to that in Tc2 cells (Fig. 5). Thus, ROG-mediated inhibition of chromatin remodeling in the IL-4 gene locus may also contribute to undetectable production of IL-4 in NK2 cells.

We detected IL-10 production in NK1 cells, but not in NK0 or NK2 cells (Fig. 1), consistent with the results of previous reports (4, 39). The mechanism underlying the NK1-cell specific expression of IL-10 is not clear at this time; however, we know that both IL-2 and IL-12 are required for the acquisition of IL-10 production in NK cells (Fig. 1) (39). Thus, some transcriptional factors induced by IL-2R- and IL-12R-mediated signaling in NK cells should be responsible for the chromatin remodeling of the IL-10 gene locus and/or IL-10 gene transcription. Differentiated NK1 cells may have immunoregulatory functions in some aspects of immune responses by the production of IL-10.

Another important finding is that the production of IL-5 and IL-13 in NK2 cells is totally dependent on STAT6 expression (Fig. 7). As shown in Fig. 3, freshly prepared NK cells express significant amounts of IL-4Rα and γC. In human NK cells, either IL-4 or IL-13 induced STAT6 phosphorylation and subsequent formation of Cε-STAT6 DNA-protein complexes (40). Thus, similar to developing Th2 cells, STAT6/GATA3-induced molecular events appear to operate in developing NK2 cells and are crucial for their differentiation and IL-5 and IL-13 production.

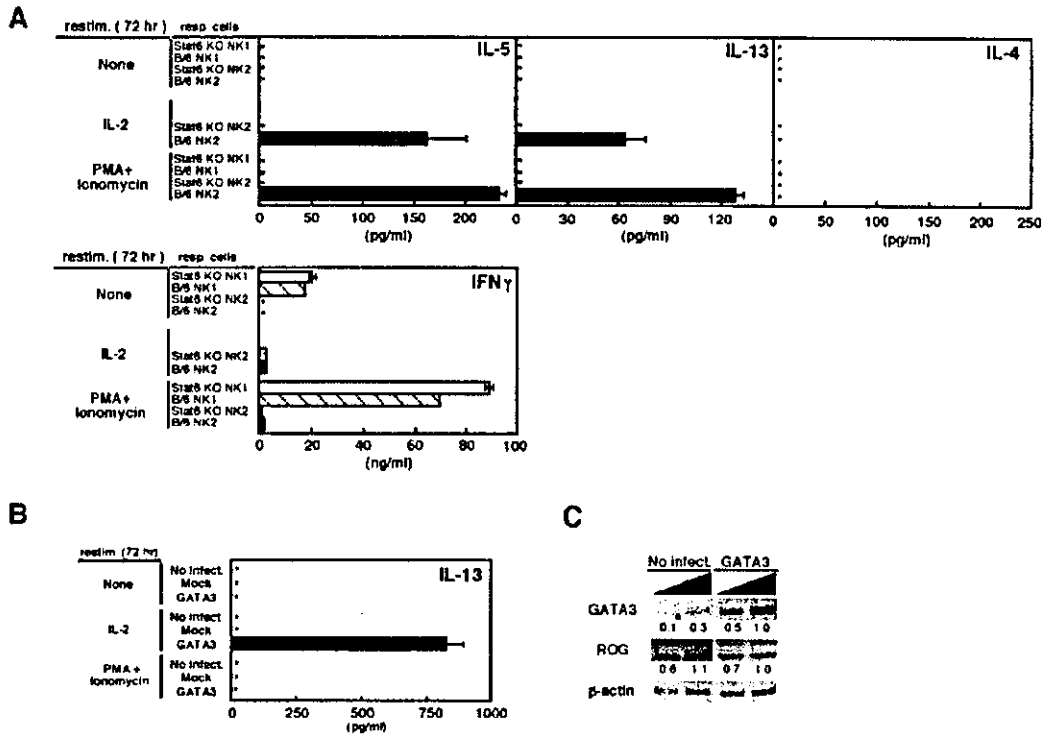

FIGURE 7. STAT6 is required for NK2 cell differentiation. *A*, NK cells from C57BL/6 and STAT6-deficient mice were cultured and restimulated as described in Fig. 1*A*. The amounts of IL-5, IL-13, IL-4, and IFN-γ in the supernatant were measured by ELISA. □, STAT6-deficient cells; ■, C57BL/6 cells. *B*, Ectopic expression of GATA3 induces IL-13 production in the LFD14 NK cell line. A fetal liver-derived NK like cell line, LFD14, was infected with a retrovirus encoding GATA3 bicistronically with EGFP. Two days after infection, EGFP-positive cells were isolated by cell sorting. After another 2 days of culture, cells were harvested and restimulated with IL-2 or PMA plus ionomycin for 72 h. The production of type 2 cytokines was measured by ELISA. *C*, Total RNA was extracted from the retrovirus-infected LFD14 cells, and the mRNA levels of ROG and GATA3 were determined by RT-PCR analysis. The relative band intensities were normalized to β-actin and are indicated under each band. *, Not detectable.

In our in vitro differentiated NK1 cells, the IFN-γ promoter locus was found to be hyperacetylated compared with that in fresh NK cells and NK2 cells. The levels were higher than those in naive CD4 T cells or Th2 cells (Fig. 6). These results are consistent with the abundant production of IFN-γ in NK1 cells.

In established NK2 cells, IL-2 restimulation induced significant amounts of IL-5 and IL-13 (Fig. 1). This is not the case in established Th2 cells, for which TCR stimulation is required for the induction of type 2 cytokine production. These results suggest that the signaling pathways downstream of IL-2R are distinct in NK2 cells. This could also be true for the signaling pathways responsible for IFN-γ production in NK1 cells (Fig. 1). In particular, IL-18 induced large amounts of IFN-γ in NK1 cells (Fig. 2).

The cytotoxic activity against K562 cells has been reported to be similar for IFN-γ-producing NK cells and nonproducing NK cells in human systems (6). We observed significant differences in cytotoxic activity among freshly prepared NK, NK0, NK1, and NK2 cells (Fig. 4). However, there appears to be no clear link between the production of IFN-γ and the cytotoxic activity of NK cell populations. CD94 was expressed only on NK1 cells, and marginal expression of Ly49A and Ly49D was found on all subsets of NK cells (Fig. 3*C*). Thus, it is not certain at present that the difference in cytotoxicity among NK0, NK1, and NK2 cell subsets can be explained by the difference in expression of these NK receptor molecules. The mRNA expression of perforin 1 and granzyme B was equivalent among these NK cell subsets (Fig. 5).

The levels of IL-12Rβ2 expression in human NK1 cells are reported to be higher than those in NK2 cells (4). However, we detected a slightly decreased expression of IL-12Rβ2 in differentiated mouse NK1 cells (Fig. 5). After differentiation, the levels of IL-2Rβ and Cγ expression were slightly lower in NK1 cells compared with NK0 and NK2 cells, whereas the others were equivalent (Fig. 3). Thus, it is not clear whether the direction of NK cell differentiation is influenced by the expression levels of certain cytokine receptor components.

Recently, Loza and Perussia (41, 42) proposed a pathway for linear 2-0-1 lymphocyte development in NK cells based on experimental results in the human NK cell system. According to their hypothesis, type 2 cells develop into type 0 cells, and then develop further into type 1 cells. Type 1 and type 2 cells do not develop from common precursor naive or type 0 cells. This is an interesting hypothesis, but our results in a mouse system do not support the hypothesis. First, we detected no type 2 cytokine-producing cells in the freshly prepared mouse NK cells (Fig. 1). Secondly, NK2 cells producing IL-5 and IL-13 were generated only when the freshly prepared NK cells were stimulated with PMA plus ionomycin in the presence of IL-2 and IL-4 for 2 days after cultivation with IL-2 and IL-4. Without IL-4 (NK0 conditions), no IL-5- and IL-13-producing cells were generated, although the number of cells at the end of the culture was about twice that in NK2 cultures (T. Nakayama and T. Katsumoto, unpublished observations).